



Ultrasound scanning of the pelvis and abdomen for staging of gynecological tumors: a review

D. FISCHEROVA

Gynecological Oncology Centre, Department of Obstetrics and Gynecology, First Faculty of Medicine and General University Hospital, Charles University, Prague, Czech Republic

KEYWORDS: cervical cancer; endometrial cancer; gynecological oncology; ovarian cancer; staging; ultrasound; vaginal cancer; vulvar cancer

ABSTRACT

This Review documents examination techniques, sonographic features and clinical considerations in ultrasound assessment of gynecological tumors. The methodology of gynecological cancer staging, including assessment of local tumor extent, lymph nodes and distant metastases, is described.

With increased technical quality, sonography has become an accurate staging method for early and advanced gynecological tumors. Other complementary imaging techniques, such as computed tomography and magnetic resonance imaging, can be used as an adjunct to ultrasound in specific cases, but are not essential to tumor staging if sonography is performed by a specialist in gynecological oncology.

Ultrasound is established as the method of choice for evaluating local extent of endometrial cancer and is the most important imaging method for the differential diagnosis of benign and malignant ovarian tumors. Ultrasound can be used to detect early as well as locally advanced cancers that extend from the vagina, cervix or other locations to the paracolpium, parametria, rectum and sigmoid colon, urinary bladder and other adjacent organs or structures. In cases of ureteric involvement, ultrasound is also helpful in locating the site of obstruction. Furthermore, it is specific for the detection of extrapelvic tumor spread to the abdominal cavity in the form of parietal or visceral carcinomatosis, omental and/or mesenteric infiltration.

Ultrasound can be used to assess changes in infiltrated lymph nodes, including demonstration of characteristic sonomorphologic and vascular patterns. Vascular patterns are particularly well visualized in peripheral nodes using high resolution linear array probes or in the pelvis using high-frequency probes. The presence of peripheral

or mixed vascularity or displacement of vessels seems to be the sole criterion in the diagnosis of metastatic or lymphomatous nodes.

In the investigation of distant metastases, if a normal visceral organ or characteristic diffuse or focal lesions (such as a simple cyst, hepatic hemangioma, renal angiomyolipoma, fatty liver (steatosis)) are identified on ultrasound, additional examinations using complementary imaging methods are not required. If, however, less characteristic findings are encountered, especially when the examination result radically affects subsequent therapeutic management, an additional examination using a complementary imaging method (e.g. contrast-enhanced ultrasound, computed tomography, magnetic resonance imaging, positron emission tomography) is indicated. Copyright © 2011 ISUOG. Published by John Wiley & Sons, Ltd.

INTRODUCTION

Ultrasound is a non-invasive, commonly available, affordable imaging method associated with minimal risk and discomfort to the patient. When performed by an experienced diagnostician, it can play an invaluable role in the primary diagnosis of gynecological cancers, the assessment of tumor extent in the pelvic and abdominal cavity and the evaluation of treatment effects as well as follow-up after treatment. Using ultrasound to evaluate important prognostic parameters makes the individualization of oncology treatment possible. In this way we can make maximum therapeutic impact with minimal patient morbidity. Ultrasound also enables the targeted biopsy of advanced tumors or metastatic lesions, allowing fast and minimally invasive establishment of the tumor histology¹.

Correspondence to: Dr D. Fischerova, Department of Obstetrics and Gynecology, First Faculty of Medicine and General University Hospital, Apolinarska 18, 12851 Prague 2, Czech Republic (e-mail: daniela.fischerova@seznam.cz)

Accepted: 8 April 2011

The accuracy of ultrasound is largely dependent on three variables: operator, equipment and patient. To become an ultrasound expert in gynecological oncology requires adequate practical expertise, which is developed through exposure to abnormal findings. It is of utmost importance to use complementary imaging methods in questionable cases and/or to be present in the operating theater in order to maximize one's knowledge of the tumor's characteristics and spread.

To examine the oncology patient, a high-end ultrasound machine equipped with sensitive Doppler and endocavitary (microconvex) and transabdominal (convex array probe for abdomen and linear probe for peripheral lymph node assessment) transducers is needed. In addition, the ultrasound findings should be stored, in the form of static images taken in standard sections, videoclips or three-dimensional volumes, for subsequent additional offline analysis, if necessary in consultation with an expert.

The last significant variable is the patient. Although over the last few years there has been considerable improvement in scanning technology, there are still limitations in some cases (e.g. obese patients and retroperitoneum evaluation, extensive ascites and liver assessment, postoperative adherent intestinal loops causing acoustic shadowing). In such cases a complementary imaging method or diagnostic laparoscopy can be used to obtain further information, if this is relevant to the patient's management.

ULTRASOUND EXAMINATION TECHNIQUE

All gynecological oncology patients should be examined systematically and carefully using a combination of endocavitary sonography, with a microconvex array probe inserted transvaginally or transrectally (Figure 1), and transabdominal sonography, with a convex array probe for evaluation of possible tumor spread in the abdominal cavity and with a linear array probe for examining the peripheral lymph nodes (Figure 2).

Transvaginal ultrasound is the optimal approach for examining the uterus (including uterine zonal anatomy: cervix, endometrium, junctional zone (endometrial/myometrial border), myometrium, perimetrium), the adnexa and the pelvic peritoneum (Figure 3, Table S1). Transrectal insertion of the probe has an advantage in patients who are virgo intacto, have a stenotic vagina or have undergone brachytherapy, in whom transvaginal insertion is not possible (Videoclip S1). However, the main use of the transrectal approach is for the detection of locally advanced tumors of the vulva, as well as early and advanced vaginal and cervical cancer (Figure 4, Table S1, Videoclip S2). In these cases, the transrectally inserted probe allows for the detection of tumor spread into the paracolpium, parametrium, and vesicocervical, vesicovaginal and rectovaginal spaces and the urinary bladder and rectum. Transrectal sonography also eliminates the risk of bleeding from an exophytically growing tumor of the vagina or uterine cervix. The technique does not

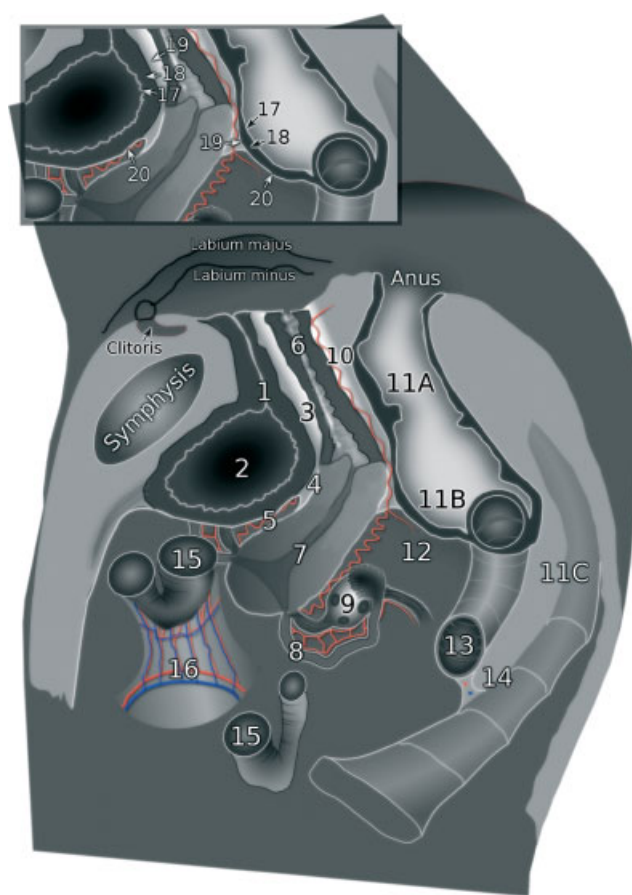


Figure 1 Pelvic anatomy as seen on transvaginal or transrectal sonography (sagittal view) during probe insertion, including details of bladder and rectal wall. 1, Urethra; 2, bladder; 3, ureterovaginal space; 4, vesicocervical space; 5, vesicouterine pouch; 6, vagina; 7, uterus; 8, Fallopian tube; 9, ovary; 10, rectovaginal space; 11, rectum (11A, retroperitoneal part; 11B, intraperitoneal part; 11C, mesorectum); 12, pouch of Douglas (rectouterine pouch); 13, sigmoid colon; 14, sigmoid mesocolon; 15, small intestine (ileum); 16, mesentery of small intestine (root of mesentery); 17, mucosa; 18, muscular layer; 19, rectal visceral fascia; 20, serosa (a reflection of the peritoneum).

require any special bowel preparation such as an enema or glycerine suppository. The patient is informed about the transrectal insertion of the probe, and the procedure is then performed with the patient in an identical position (supine, with elevated pelvis) and with an identical probe to that used for a transvaginal procedure. Guiding the probe into the rectum via the anus is accomplished through coordinated movement of the probe in the examiner's right and left hands. The index finger of the left hand opens the anus by exerting gentle pressure on the base of the posterior commissure while the probe is inserted into the anus by gently depressing the anterior commissure. If the anal sphincter is constricted, the patient may be instructed to perform the Valsalva maneuver.

For transabdominal sonography, a convex array probe (3.5–7 MHz) is usually used, depending on the patient's body habitus. An ultrasound examination of the abdominal cavity has to be performed systematically and the entire anatomy has to be evaluated in both sagittal and transverse sections, which is accomplished by rotating

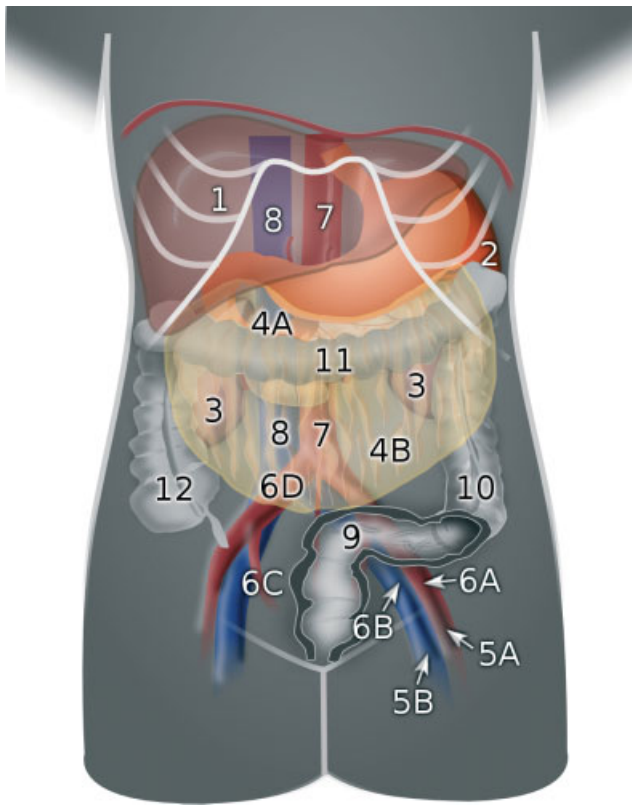


Figure 2 Anatomy as seen on transabdominal sonography, with evaluation of visceral organs, peritoneal surfaces including omentum and lymph nodes surrounding the main and visceral vessels. 1, liver; 2, spleen; 3, kidney; 4, greater omentum (4A, supracolic part; 4B, infracolic part); 5, femoral vessels (5A, femoral artery; 5B, femoral vein); 6, iliac vessels (6A, external iliac artery; 6B, external iliac vein; 6C, internal iliac artery; 6D, common iliac artery); 7, aorta; 8, inferior vena cava; 9, sigmoid colon; 10, descending colon; 11, transverse colon; 12, ascending colon.

the probe 90°. It is helpful to memorize the order of the steps needed to complete a full transabdominal ultrasound examination to ensure it is performed identically each time and thus prevent any omissions. First, attention is paid to the visceral organs in the upper abdomen (such as the kidneys and adrenal glands, spleen, liver and pancreas); their size and structure is evaluated and possible intraparenchymatous focal or diffuse lesions, capsular infiltration or visceral lymphadenopathy are described (Figure 5). Second, the parietal, visceral, mesenteric peritoneum and omentum are evaluated, as there is potential for tumor spread in the form of parietal (lateral paracolic gutters, diaphragm, anterior abdominal wall), omental, visceral (intestinal carcinomatosis, organ surfaces) or mesenteric (mesentery of small intestine or mesocolon) carcinomatosis. Finally, the peripheral (superficial and deep inguinal) and retroperitoneal (also called parietal) lymph nodes are evaluated. In experienced hands, the usual duration of a systematically performed combination of transvaginal (or transrectal) and transabdominal scans to define the clinical stage of disease is approximately 15 min.

Ultrasonography is a dynamic procedure during which the possibility of additional functional tests can provide important information (Videoclip S3)². The acoustic

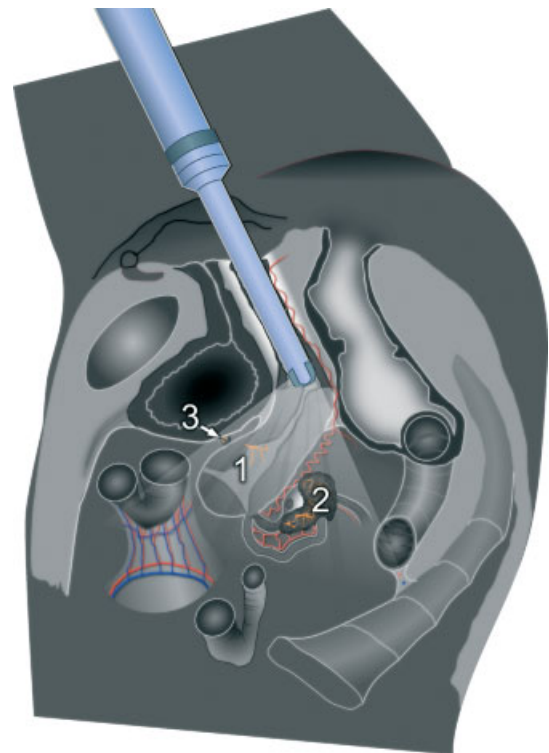


Figure 3 Examples of indication for transvaginal sonography. 1, Uterine tumor; 2, adnexal mass; 3, peritoneal tumor.

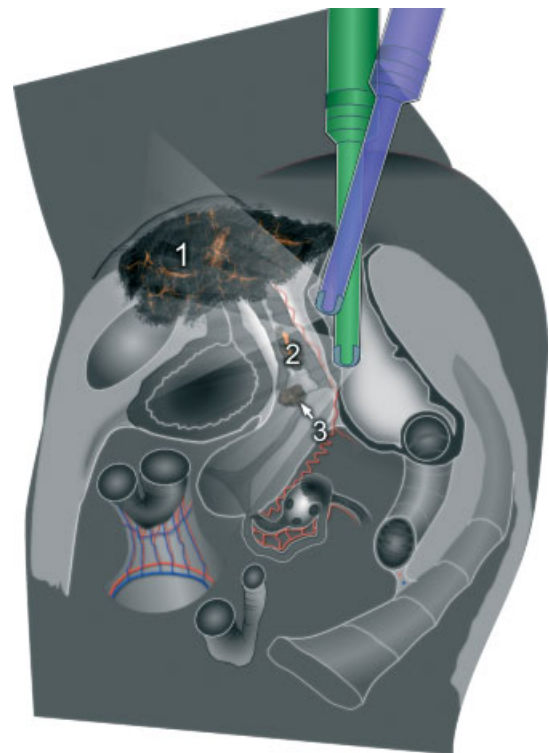


Figure 4 Examples of indication for transrectal sonography. 1, Advanced vulval cancer; 2, vaginal cancer; 3, cervical cancer.

visibility of organs located partially within the rib cage may be improved by deep inspiration and slow expiration. The patient also provides important information on tenderness during the examination (e.g. level of pain

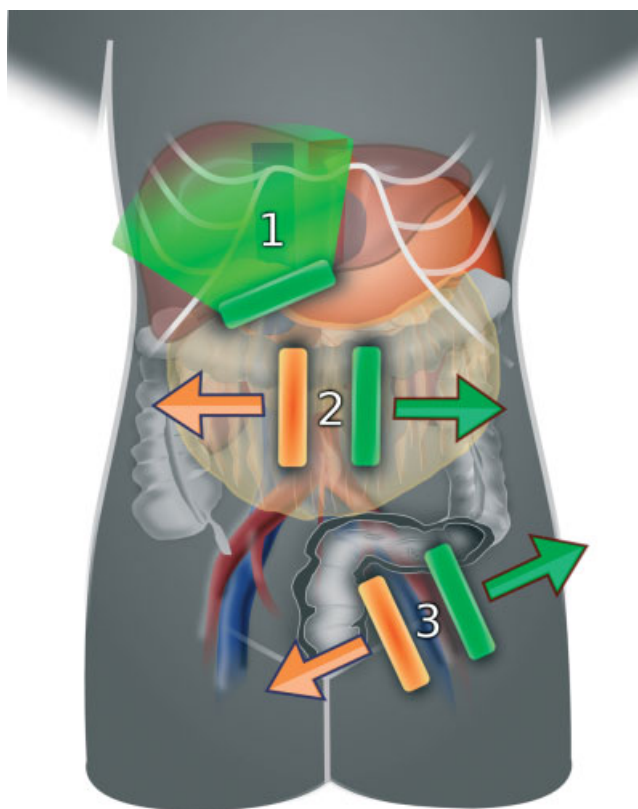


Figure 5 Steps involved in transabdominal sonography. 1, Evaluation of visceral organs; 2, assessment of peritoneal surfaces, including omentum; 3, detection of inguinal and retroperitoneal lymphadenopathy. Probe position is indicated by orange and green bars and probe movement by arrows.

during vaginal examination of various pelvic structures, sonopalpation of liver to determine a dull pain due to the involvement or stretching of the liver capsule in the event of metastatic spread to the liver). It is also important to evaluate the mobility of organs in order to exclude adhesions, to observe the movement of a tumor relative to an organ in order to determine the tumor origin and/or to observe movement of fluid within the pelvis or abdominal cavity or within a tumor itself. The inherent movement of the target organ may also be used, for example when assessing gallbladder content, or when trying to distinguish between intestinal loops and an infiltrated omentum based on the presence or absence of peristalsis. Intestinal peristalsis may even be provoked through repeated pressure exerted by the probe (Videoclip S3). Sonopalpation of the liver not only evaluates its tenderness (capsule tension-related pain, dull pain) provoked by contact of probe with the organ but can also assess its consistency in the event that liver cirrhosis is suspected.

Morphological characterization may be complemented by Doppler ultrasonography to assess the presence, architecture and density of newly formed vessels. Doppler is also useful to confirm the size of isoechogenic (less sonomorphologically pronounced) tumors, and to evaluate changes in tumor viability after treatment (post-irradiation or post-chemotherapy changes versus persistent viable tumor). In general the vascularization

of a tumor mirrors its biological behavior; tumors with a higher density of newly formed vessels are usually more aggressive, form lymphatic metastases early and, therefore, tend to be of a higher FIGO stage³⁻⁶. When performing a color Doppler examination, a subjective semiquantitative assessment of blood flow is made as follows: a score of 1 is given when no blood flow can be observed in the lesion; a score of 2 is given when only minimal flow can be detected; a score of 3 is given when moderate flow is present; a score of 4 is given when the mass appears highly vascularized⁷.

Another possibility that may increase the sensitivity and specificity of ultrasonography is the use of ultrasound contrast media (contrast enhanced ultrasonography), especially for the differential diagnosis of hepatic lesions. This, however, requires special ultrasound software as well as intravenous use of the suspension and, therefore, the advantages of ultrasound as a readily available, affordable and non-invasive method are compromised⁸.

PRIMARY GYNECOLOGICAL TUMORS (TNM STAGING)

When a tumor is limited to the organ of origin, special attention must be paid to a careful description of prognostic parameters essential for individualization of treatment and choice of therapeutic modality (Table S2)⁹. Ultrasound also has a role to play in the precise evaluation of advanced tumors (Table S2) that spread either locally, through infiltration of surrounding structures (paracolpium, pericervical fascia and parametria, urethra, urinary bladder, rectosigmoid), and/or in the form of peritoneal lesions in the pelvis and abdominal cavity (carcinomatosis). In addition, the tumor could also spread through the lymphatic and vascular system, as described by the TNM (primary Tumor, regional lymph Nodes and distant Metastasis) staging classification system developed by the International Union Against Cancer (UICC) and the American Joint Committee on Cancer (AJCC)¹⁰. After the T, N and M categories are assigned, they can be further grouped into Stages I–IV according to the FIGO staging system developed by the International Federation of Gynecology and Obstetrics. The revised FIGO staging published in 2009 should be used for determining the clinical and surgical staging in gynecological oncology¹¹.

Assessment of primary tumor confined to the organ of origin (T1NM)

Vaginal cancer

Method: combination of transrectal sonography in both sagittal and transverse planes

On ultrasound, the vagina is delimited ventrally and dorsally by hyperechogenic visceral fascia. These, together with vesical or rectal fasciae, form the hypoechogenic vesicovaginal and rectovaginal spaces, which are filled with areolar connective tissue. The hyperechogenic tissue

along the side of the vagina up to the level of the vaginal fornix attachment to the cervix is named the paracolpium and consists of connective mesenteries enveloping the vaginal and the inferior vesical vessels. Ultrasound should distinguish between tumors limited to the vaginal wall, i.e. Stage-I tumors, and locally advanced tumors, as the latter require more extensive treatment (Figure S1).

Cervical cancer

Method: transrectal or transvaginal sonography in sagittal and transverse planes

The sonographic detection rate for cervical cancer is 93–94%^{12,13} and ultrasound is a highly accurate method in classifying early-stage tumors^{12–15}. It is important to focus on the following information required from the ultrasound examiners by the clinicians who will be planning the individual treatment of a patient. First, the presence of a tumor and its topography/growth pattern (exocervix/exophytic tumor growth (Figure S2), endocervix/infiltrative tumor growth (Figures S3–S5)) need to be assessed. The tumor size is measured in three diameters (Figure S6). The next step is especially important for young patients requiring a fertility-sparing procedure¹⁶: it must be determined whether the distance between the tumor and the internal cervical os is sufficiently large (≥ 10 mm) to maintain an adequate tumor-free margin and reduce the risk of future miscarriage (Figure S7)^{17,18}. The third priority for an ultrasound examiner is to evaluate the extent of tumor stromal invasion. The proportion of stromal invasion can be defined as either partial ($\leq 2/3$ or $> 2/3$) or full-thickness or, more precisely, it can be defined based on the measurement of tumor-free stroma (Figure S8, Figure 6). This is achieved by measuring the distance between the tumor and the pericervix, or pericervical fascia (dense hyperechogenic tissue surrounding the cervix), at the point where the ventral (including vesicouterine and vesicovaginal), lateral and dorsal (including uterosacral and sacrovaginal) ligaments attach to the cervix on both sides. The extent of the radical procedure (parametrectomy) can then be planned, based on these data¹⁹. For example, in Figure S8, the tumor almost reaches the pericervical fascia on the right side and, therefore, extended radical parametrectomy is required. On the contralateral side, a less radical procedure is needed because the tumor does not extend into the pericervical fascia. If the pericervical fascia is infiltrated by tumor, the degree of parametrial involvement is graded according to the scale introduced in Table S3.

Endometrial cancer

Method: transvaginal sonography in sagittal and transverse planes

Ultrasound is widely accepted as the appropriate staging method for early-stage endometrial cancer⁹. Sonographic diagnosis should provide the clinician with

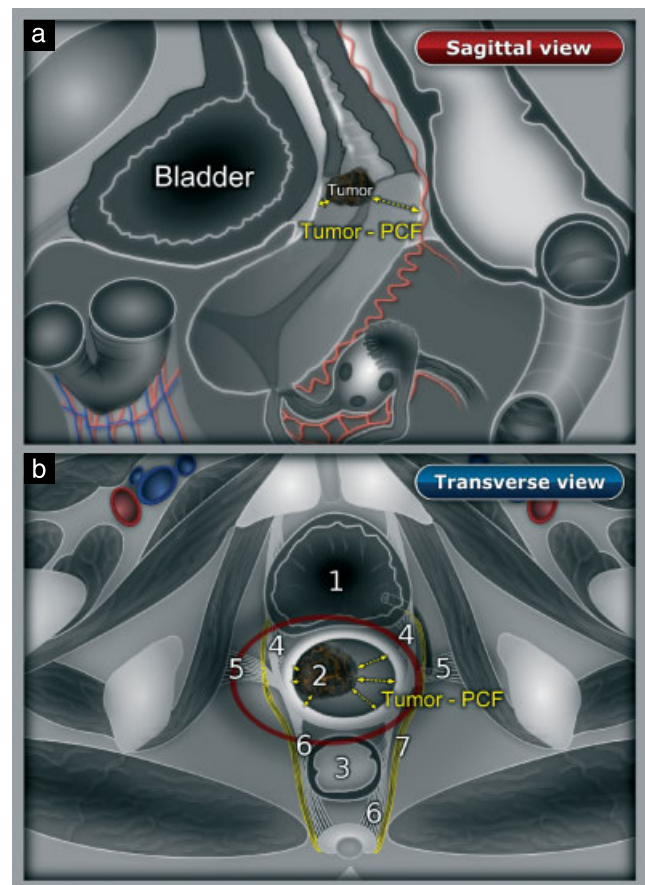


Figure 6 Transvaginal/transrectal sonographic measurement of tumor-free stroma in cervical cancer: measuring the distance between cervical tumor and pericervical fascia (PCF) allows individualization of treatment with respect to the degree of extension laterally during parametrectomy in the eccentrically located tumor. (a) Tumor–PCF measurement ventrally and dorsally in the sagittal view in eccentrically located tumor; (b) tumor–PCF measurement in transverse view. Red circle shows extent of required parametrectomy around the cervical cancer. 1, Urinary bladder; 2, cervical cancer; 3, rectum; 4, ventral parametrium; 5, lateral parametrium; 6, dorsal parametrium; 7, autonomic nerves/hypogastric plexus; dotted double-headed arrows correspond to the distances between tumor and pericervical fascia measured at points where parametria arise. Note that the parametria are accompanied by autonomic nerves that remain intact during the less radical procedure, with less serious side effects.

information regarding the tumor location, size (three diameters), sonomorphology (e.g. echogenicity, homogeneity, endometrial–myometrial junction) and vascular pattern²⁰. Moreover, it offers the possibility of evaluating the extent of tumor infiltration into the myometrium and towards the cervix. Ideally, the depth of tumor invasion should be measured from the endometrial–myometrial interface to the deepest edge of the tumor extension into the myometrium and should be related to the width of the normal myometrium. However, sonographic measurement has its limitations: in some cases the normal myometrium is not accessible as it is either consumed by the tumor or greatly thinned by pressure from exophytically grown tumor. Another means of measuring the degree of myometrial infiltration is to determine the

relationship between the maximum tumor thickness (d1) and the anteroposterior diameter of the uterus (d2) in the sagittal plane. Invasion of less than half the myometrium is recorded when the ratio of d1 to d2 is <50% (Stage T1a), and invasion equal to or greater than half the myometrium is recorded when the ratio of d1 to d2 equals or exceeds 50% (Stage T1b)²¹. This approach seems less operator-dependent, although the extent of invasion may be overestimated in cases of large polypoid exophytic tumors with intact but thinned myometrium. Both techniques have over 80% accuracy in assessing the extent of myometrial infiltration^{21–23}. Another option is to measure instead the shortest myometrial tumor-free distance to the serosa. This parameter is easily assessed and seems also to be a useful prognostic factor for recurrence, using a cut-off of 10 mm (area under the receiver–operating characteristics curve, 0.76)²⁴.

In addition, power Doppler can be useful to assess the vascular pattern. For example, the presence of abnormal perfusion permits better detection of the tumor border in less visible tumors (i.e. those that are ischoechogenic with the myometrium). The presence of adenomyosis is accompanied by normal myometrial perfusion, while a circular vessel pattern helps to differentiate myomas. Moreover, in cases of mainly polypoid growing tumors, the detection with Doppler of dominant feeding vessels enables more detailed examination of the endometrial–myometrial junction at the insertion of the pedicle (entry point of feeding artery) in order to assess more accurately the depth of myometrial invasion (Figure S9).

In order to exclude cervical stromal involvement, it is important to visualize the level of the uterine artery entries into the uterus. By shifting the probe from side to side to assess the whole uterus in the sagittal plane, the level of entry of the left and right uterine arteries can be determined by Doppler. This level corresponds approximately to the internal cervical os. In cases in which the endometrial tumor only protrudes into the cervical canal and has not infiltrated the cervical stroma, by applying slight pressure with the transvaginal probe the sliding effect of tumor mass against the endocervical mucosa can be observed. Figure 7 and Figure S10 summarize the sonographic negative prognostic factors for recurrence of endometrial cancer and eventual survival²⁵. These high-risk endometrial cancers present on ultrasound as large hypoechoic or mixed tumors located in the isthmus/fundus/whole uterus, with multiple global vessels entering them via the endometrial–myometrial border, with deep extension into the myometrium and eventually the cervical stroma²⁶ (Video-clip S4).

Tubal cancer

Method: transvaginal sonography in sagittal and transverse planes

A patient's prognosis is affected significantly if early-stage tubal cancer is properly diagnosed. As with ovarian

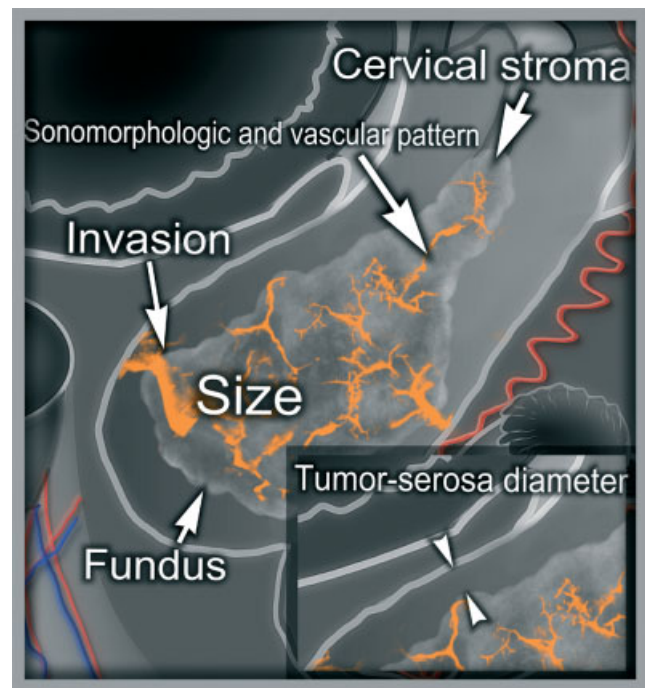


Figure 7 High-risk endometrial cancer: summary of negative prognostic factors.

tumors, but in contrast to vulval, vaginal, cervical and endometrial cancers, the biopsy results are not known prior to surgery. We must keep in mind the potential risk of tubal cancer, for example in cases of solid 'sausage-like' (Figure S11) or fibroma-like (Figure S12) perfused structures near the ovary, or in cases of hydrosalpinx containing a solid area with rich vascularity (Figure S13) (Figure 8).

Ovarian cancer

Method: transvaginal sonography in sagittal and transverse planes

High-quality ultrasound is, in most cases, the imaging method of choice with respect to the characterization of adnexal masses. Increased size, the presence of solid papillary projections, a high color score as well as the presence of a highly vascularized solid component within an adnexal mass are all findings that may be associated with a diagnosis of malignancy (Figures S14 and S15). The optimal method for assessing the likely pathology of a pelvic mass is ultrasonography by an expert; however, mathematical models have been developed that have performed to a similar level on external validation²⁷. When considering fertility-sparing surgery, using ultrasound to exclude the possibility of tumor spread through the ovarian capsule and to confirm that the contralateral ovary is normal may allow the contralateral ovary to be left *in situ* without the need for an intraoperative biopsy (Figure S16).

Assessment of tumor extension (T2–T4NM)

Whilst ultrasound has been accepted as the technique of choice for the assessment of gynecological tumors

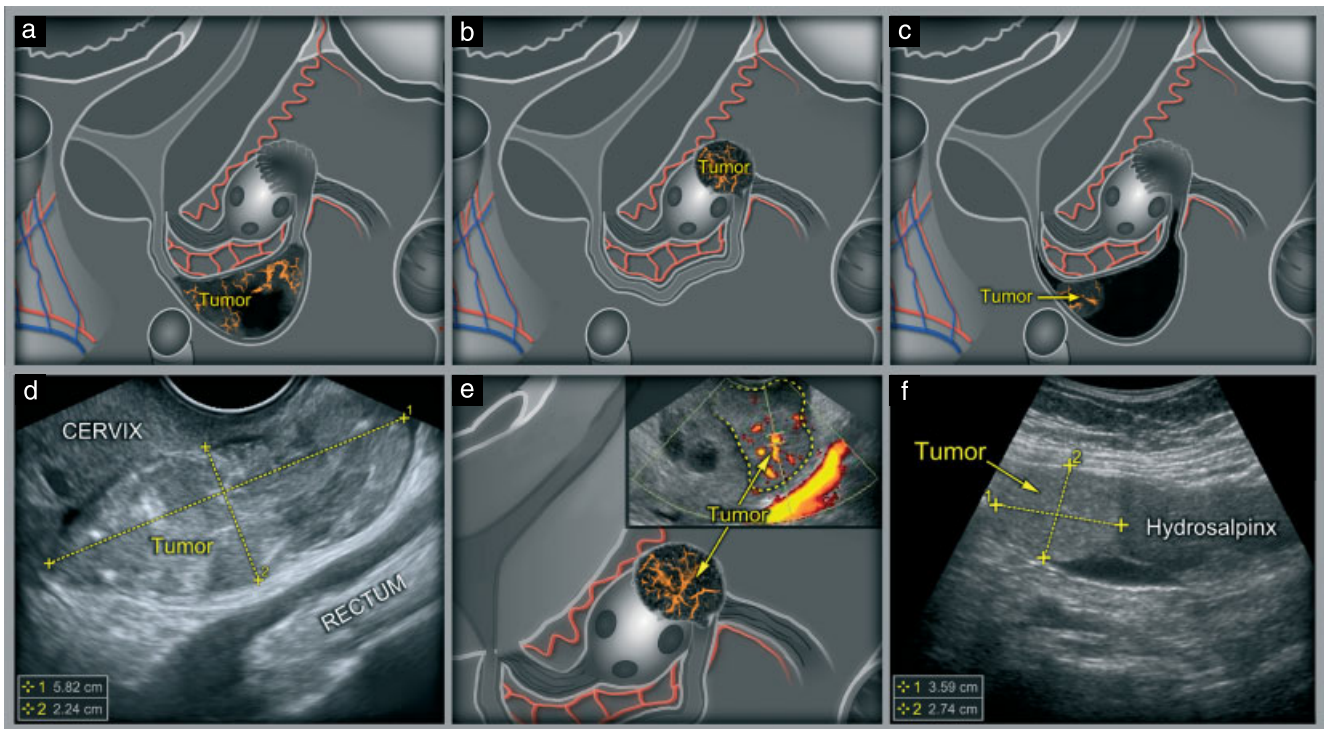


Figure 8 Examples of tubal cancer as seen on transvaginal sonography. Schematic diagrams (a–c) with corresponding ultrasound images (d–f) showing: (a,d) early tubal cancer manifested as solid ‘sausage-like’ perfused structure near the ovary; (b,e) perfused solid lesion close to the ovary (note, in contrast to a fibroma, this lesion is highly perfused and lacks echogenic stripes); (c,f) hydrosalpinx with a concurrent solid vascularized lesion.

limited to the organ of origin, it is becoming increasingly recognized that ultrasound is important for individual treatment planning in locally advanced gynecological tumors involving adjacent pelvic organs, as well as for assessing tumor extent within the abdominal cavity, when in the hands of an experienced ultrasound examiner. There is a significant amount of evidence relating to ultrasound examination of early-stage gynecological tumors. Much less has been published about sonography of more advanced tumor stages, which will, thus, be the focus of the information provided below.

Infiltration of the paracolpium

Method: transrectal sonography in sagittal and transverse planes

In the event of tumor spread into the vagina or when a primary vaginal tumor is diagnosed, it is important for surgical planning to determine whether the tumor is limited to the vaginal wall or whether it has already penetrated the visceral fasciae ventrally or dorsally and is growing into the vesicovaginal/rectovaginal space and/or is invading the surrounding tissues (paracolpium) laterally. The presence of hypoechoic tumor prominences into the hyperechoic connective tissue of fasciae or paracolpium should be assessed in both transverse and sagittal views on transrectal sonography (Figure S1, Figure 9). Although the term paracolpos is frequently used in pelvic oncology surgery, this structure is not officially recognized in the international anatomical nomenclature and is classified as part of the paracervix^{28,29}.

Parametrial infiltration

Method: transrectal sonography or transvaginal sonography in both sagittal and transverse planes

Assessment of parametrial infiltration must be approached in a standardized manner. It is useful to start with a midsagittal plane at the level of the ectocervix up to the uterine isthmus; the probe is then gradually moved to the right from the midline (Figure S17a–c, Videoclip S5) to observe the ventral, dorsal and lateral right parametria. Next, the probe is moved backwards in the same way and continues from there to the left side of the pelvis (first step). Rotating the probe through 90° counterclockwise and shifting from the urinary bladder towards the rectum (Figure S17d–f) shows the urinary bladder wall, the ventral parametria, the cervix and lateral and dorsal parametria and the rectum (second step) (Figure 10).

Standard clinical examination of the parametrium usually gives inaccurate results, especially in cases of incipient parametrial infiltration in obese patients or patients with bulky tumors. In contrast, the accuracy of transrectal sonography for the detection of parametrial involvement is comparable to that of MRI (98.9% vs 94.7%, $P \leq 0.219$)¹². For clinical purposes it is important to discern whether the pericervical fascia is infiltrated, and to describe the topography precisely. Currently, we are advised to use the international anatomical nomenclature, although this is not always what happens in the surgical literature and in daily use^{28–30}. In international anatomical nomenclature, ‘parametrium’ refers to tissues that surround the uterine artery between

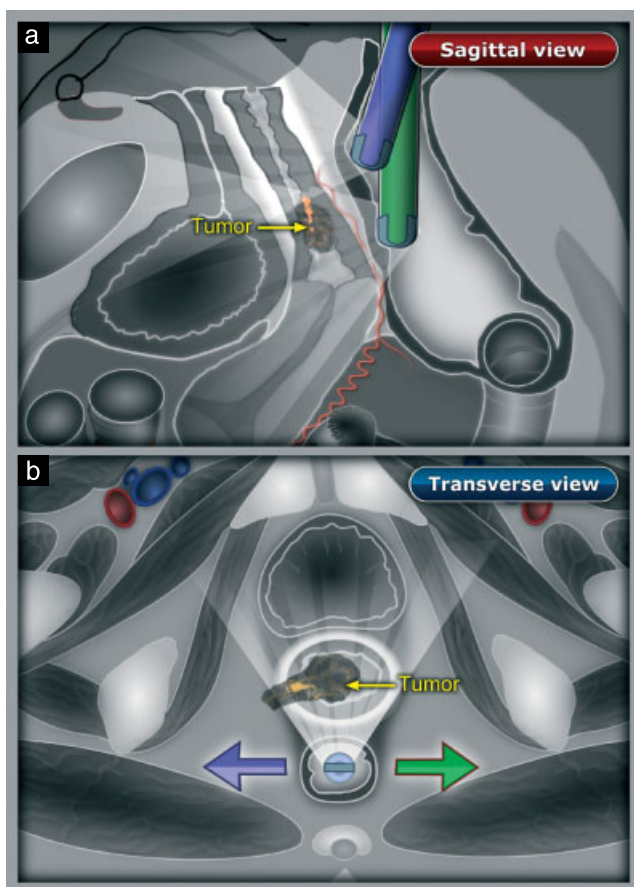


Figure 9 Vaginal cancer as seen on transrectal sonography in sagittal (a) and transverse (b) views. Along with ventral and dorsal shifting, the probe is also usually moved slightly to the right or left towards an area of interest. The arrows in (b) indicate movement of the probes shown in (a). Note that in the sagittal view, the cancer does not seem to be infiltrating the vaginal wall; however, the transverse view confirms that the tumor extends to the paracolpium.

the uterine corpus and pelvic sidewall cranial to the ureter and superficial uterine pedicle. The dorsolateral attachment of the cervix is named the ‘paracervix’, and this term should replace others such as cardinal ligaments, ligaments of Mackenrodt, lateral cervical ligaments and parametrium. Moreover, cervical cancer can spread in

any direction, ventrally affecting the vesicouterine and vesicovaginal ligament (otherwise referred to as ventral parametrium) and/or dorsally affecting the uterosacral and sacrovaginal ligament (otherwise referred to as dorsal parametrium). Although the consensus of new anatomical terminology was reached more than 10 years ago, surgeons are reluctant to abandon the unofficial but traditional terminology (ventral, lateral and dorsal parametrium)³¹.

Because precise evaluation of the extent of parametrial tumor involvement into ventral/lateral/dorsal parametria is so important for clinical practice, we adopted a five-level grading scale to assist in treatment planning (Figures S18–S20, Table S3, Figure 11). The well-defined hyperechogenic line surrounding the cervical stroma is described on ultrasound as the pericervix or pericervical fascia. However, on the lateral sites where the lateral parametrium is attached to the cervix and the uterine and other parametrial vessels enter the cervix, the pericervical fascia is not properly visualized. At this point the parametrial involvement is manifested as hypoechogenic irregular tumor prominences into the lateral parametrium, which has to be differentiated from the cervical vascular plexuses using color or power Doppler. In the case of advanced cervical cancer, we must distinguish whether the tumor only infiltrates the pericervical fascia (Grade 1), whether it progresses continuously through the pericervical fascia to the parametrium (Grade 2–3), or whether it spreads non-continuously in the form of ‘skip’ metastases in the lateral parametrium (Grade 4). Skip metastases (i.e. visceral parauterine lymph node metastases) are pictured as hypoechogenic rounded lesions that need to be evaluated in both sagittal and transverse planes to avoid confusing them with the hypoechogenic image of cervical vascular plexuses. In addition to their precise topography, the size of infiltrated parametrial ligaments is measured in three directions.

Involvement of urinary bladder

Method: transrectal or transvaginal sonography in sagittal and transverse planes

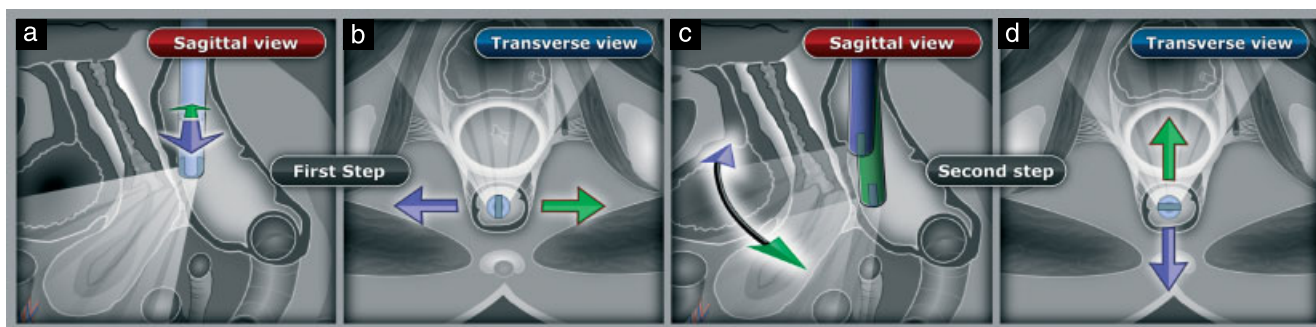


Figure 10 Technique of parametrial evaluation by transrectal sonography in sagittal and transverse views. (a) First step, sagittal view: shifting of the probe (blue and green arrows) from midline to right and left; (b) first step, transverse view; (c) second step, sagittal view: rotation of the probe 90° counterclockwise and evaluation of parametria by shifting the probe from bladder towards rectum; (d) second step, transverse view. Note that, along with ventral and dorsal shifting, the probe is also usually moved slightly to the right or left towards an area of interest, i.e. either the right or the left parametrium.

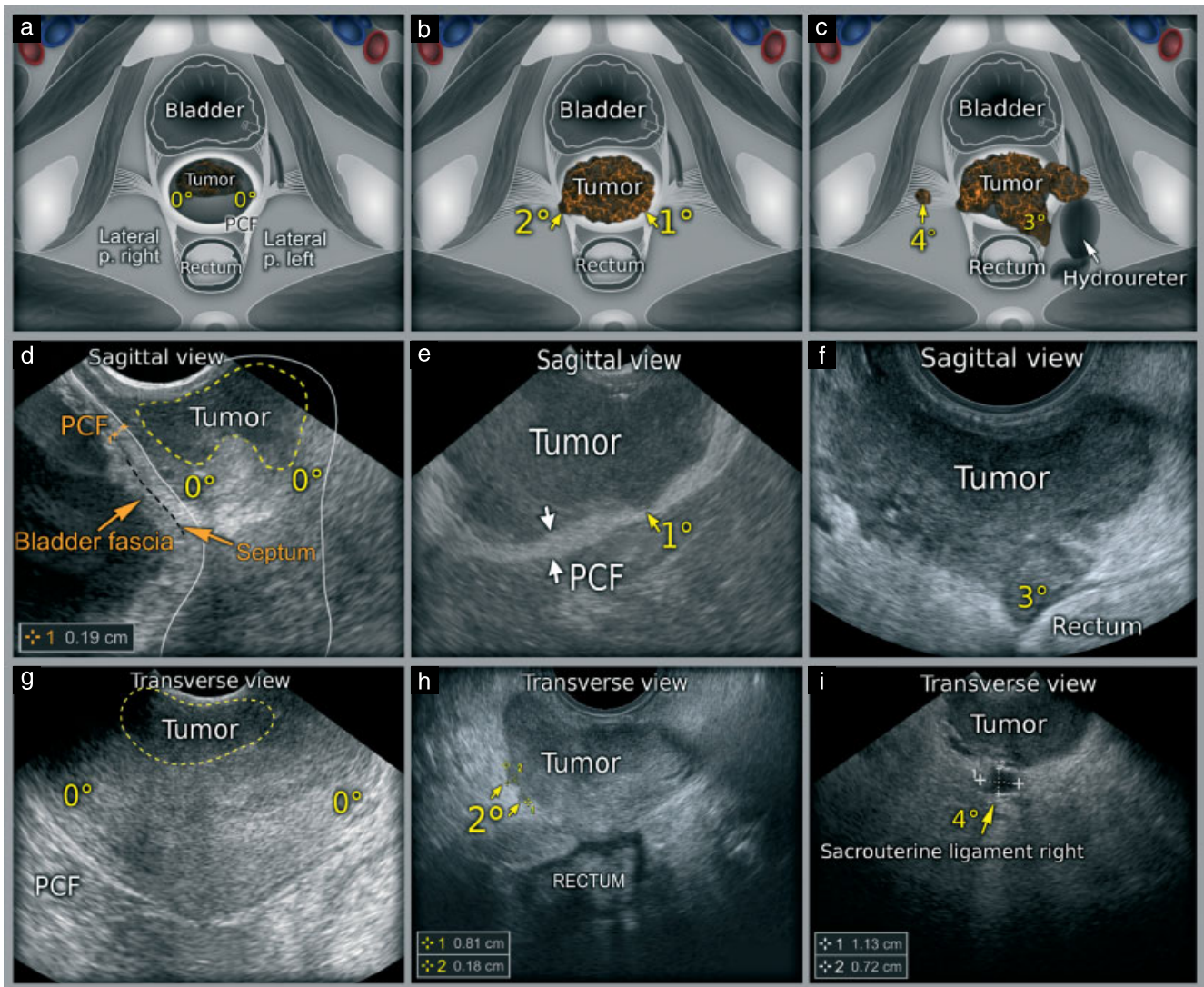


Figure 11 Grading of parametrial infiltration by transvaginal/transrectal sonography. (a–c) Schematic diagrams showing: (a) intact pericervical fascia (PCF) (Grade 0), lateral parametria (lateral p.) and PCF; (b) parametrial infiltration Grade 1 (disrupted PCF but without progression through the fascia into parametria) and Grade 2 (incipient infiltration of PCF); note that the incipient infiltration is characterized by discrete breaks in the PCF with very fine hypoechoic prominences into the parametria; (c) nodular infiltration (Grade 3) and discontinuous parametrial infiltration (Grade 4). (d–i) Ultrasound images showing: (d) in the sagittal view, hyperechoic PCF (Grade 0) located between the cervix and hyperechoic bladder visceral fascia (black dashed line corresponds to the vesicocervical space also known as the septum); (g) in the transverse view, intact PCF surrounding the cervical stroma dorsally; (e,f,h,i) parametrial infiltration Grades 1–4.

The extent of primary tumor spread into the urinary bladder and/or rectum can be determined simultaneously and the level of infiltration in both is graded identically (Figure 12). Ultrasound provides more detailed information on bladder involvement than does cystoscopy, as this can only show bullous mucosal edema in the case of tumor infiltration reaching the submucosa, or polypous changes of the urinary bladder mucosa. In clinical practice, different classifications are established with regard to the depth of tumor invasion³². It seems to be sufficient to distinguish whether the tumor reaches the external (or outer) hyperechoic layer of the bladder, which corresponds to the vesical fascia, or continues to spread into the hypoechoic bladder wall muscle layer, or whether it grows into the hyperechoic mucosa. We adopted this three-point invasion score and present it in Table S4 and in Figures S21–S23.

In addition, an evaluation of the integrity of the urinary bladder wall can be obtained through a functional test, whereby exerting pressure with the probe on the anterior vaginal wall determines the mobility (sliding) of the bladder against the uterine cervix².

Rectum/rectosigmoid infiltration

Method: transrectal or transvaginal sonography in sagittal and transverse planes

While in clinical practice the ultrasound staging of rectal carcinoma requires a precise evaluation of the tumor spread through different layers of the rectal wall towards the mucosa, in gynecological oncology a simpler classification scheme is sufficient. This resembles the one used for description of tumor spread through the urinary bladder wall (Table S4, Figure 12).

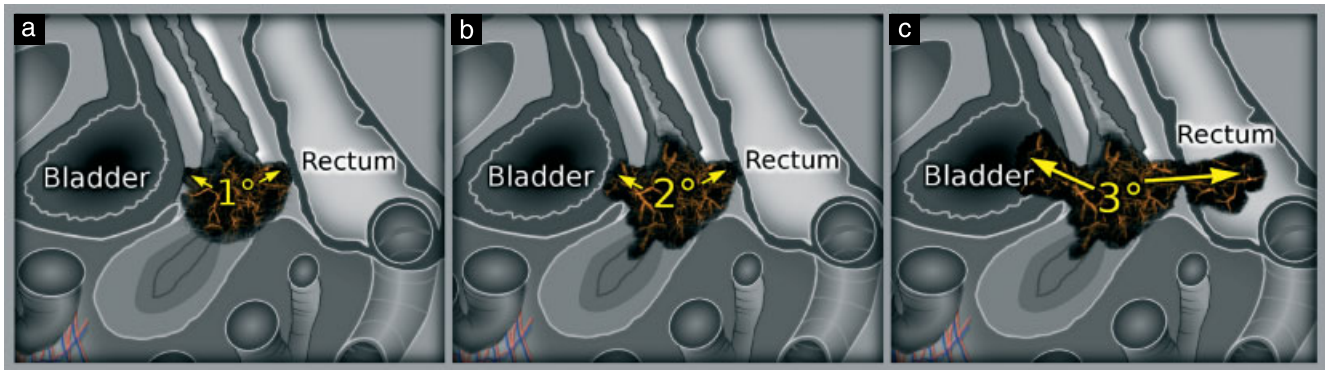


Figure 12 Grading of bladder and/or rectal tumor infiltration as seen on transvaginal/transrectal sonography. (a) Grade 1 (infiltration of hyperechogenic bladder and/or rectal fascia); (b) Grade 2 (infiltration of hypoechoogenic muscle layer); (c) Grade 3 (infiltration of hyperechogenic mucosa and intraluminal tumor nodule).

In healthy individuals, all pelvic organs are demarcated subperitoneally against the rectal wall by a narrow echogenic stripe of fibrous and fat tissue: the visceral fascia. Gynecological tumors (from vagina, cervix and other locations) infiltrate first the hyperechogenic layer that reflects their visceral fascia, then the hypoechoogenic rectovaginal space (also known as rectovaginal septum, posterior vaginal fascia or Denonvillier’s fascia) that extends inferiorly between the cervix and vagina (ventrally) and the rectum (dorsally). Subsequently, the tumors spread through the hyperechogenic rectal fascia into its hypoechoogenic muscular layer and hyperechogenic mucosa into the lumen (Figures S24–S26, Table S5). As with urinary bladder wall infiltration, knowing the extent of rectal wall involvement could modify management, for example choice of radiotherapy type that will reduce the risk of organ fistula development.

After emerging from the pouch of Douglas, the rectum is no longer positioned subperitoneally; it is surrounded by peritoneum that could form a mesorectum and, at about 15–20 cm from the anus in the mid-sacral region, it reaches the sigmoid colon where it is still wrapped in the peritoneum that now forms the sigmoid mesocolon, attaching the sigmoid colon to the posterior abdominal wall (Figure 1). Advanced tumors of the ovary and Fallopian tubes, and primary peritoneal tumors not only spread along the subperitoneally positioned rectal wall, where they usually infiltrate the rectovaginal space (Figure S24b,c), but also reach the peritoneal surface of the rectum and the sigmoid in the form of metastatic implants, with infiltration of the intestinal hyperechogenic layer (serosa), hypoechoogenic layer (more deeply located muscle layer), or, in rare cases, the intestinal mucosa, where they bulge into the lumen of the intestine (Figure S27). Knowing whether the wall of the rectosigmoid is infiltrated by an advanced ovarian cancer is essential when planning the extent of primary cytoreductive treatment.

Hydroureter and hydronephrosis

Method: combination of transvaginal and transabdominal sonography in both sagittal and transverse planes

Especially in locally advanced cervical cancers, extrinsic obstruction of the distal part of a ureter may be encountered (Figure S20d). The ureter can become compressed or infiltrated where it touches the vasa iliaca in the event of massive lymphadenopathy, or through tumor infiltration of the ventral/lateral/dorsal parametrium. If the obstruction is in the vicinity of the bladder, the megaureter and its peristalsis will eventually be visualized by an endocavitary probe inserted transvaginally or transrectally (Videoclip S6). Transabdominal ultrasonography can be used to follow a dilated ureter from the kidney to the pelvis.

Ureteral dilatation may be accompanied by distention of the renal sinus (Grade 1, Figure S28), distention of the renal pelvis and calyces (Grade 2, Figure S29) and by sacciform hydronephrosis followed by atrophy of the renal parenchyma (Grade 3, Figure S30a,b, Figure 13). The degree of hydronephrosis depends on the duration and type of the obstruction (partial or complete) (Table S6). In advanced cervical cancer, hydronephrosis is usually an asymptomatic finding and may be either uni- or bilateral, depending on the type of parametrial infiltration. Transabdominal ultrasound is an efficient method for assessing the presence or absence of hydronephrosis. In certain cases, the dilated ureter is visualized as far as the pelvis, but from that point onwards it is more advantageous to use an endoluminal probe to identify partial or complete ureteral obstruction in detail (Figure S30c). High accuracy in the sonographic diagnosis of hydronephrosis and possibly also identification of location of the obstruction allows for timely intervention in order to prevent the development of a non-functional kidney.

Implant metastases (carcinomatosis)

Method: combination of transvaginal and transabdominal sonography in both sagittal and transverse planes

The peritoneum that lines the walls of the abdominopelvic cavity (parietal peritoneum) invaginates at certain points, with an organ inside each invagination (visceral peritoneum). If this invaginated peritoneum comes in contact with itself, it forms the organ’s mesentery. For example, the mesentery suspends the jejunum

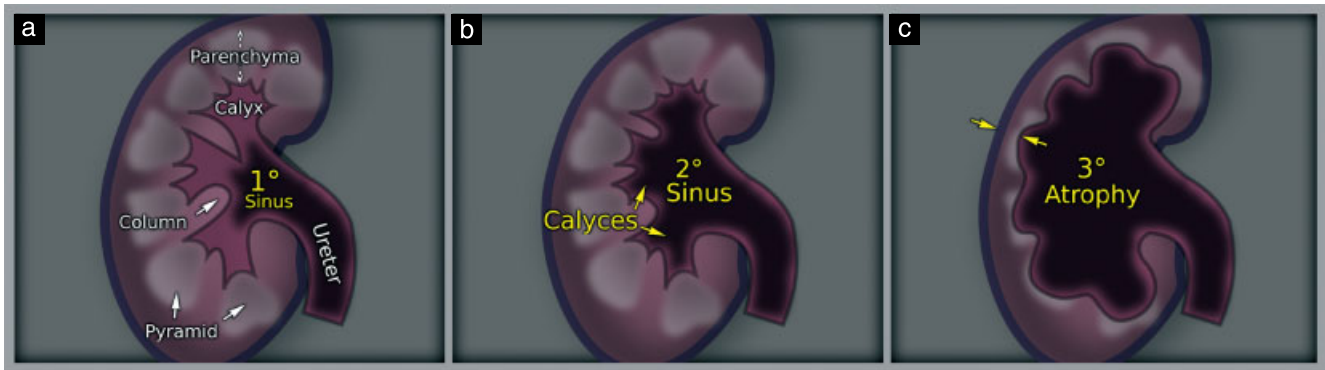


Figure 13 Hydronephrosis as seen on transabdominal sonography. (a) Grade 1 (dilation of renal sinus); (b) Grade 2 (dilation of renal sinus and calyces); (c) Grade 3 (sacciform dilation of renal sinus and calyces accompanied by renal parenchyma atrophy).

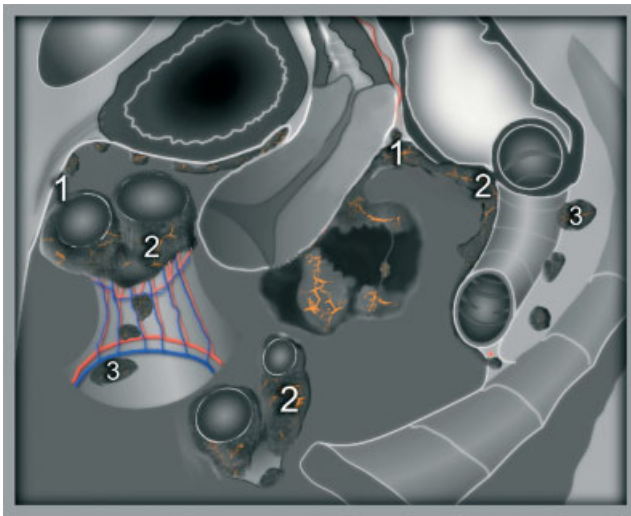


Figure 14 Schematic illustration of types of pelvic carcinomatosis. 1, Parietal carcinomatosis; 2, visceral carcinomatosis; 3, mesenteric carcinomatosis.

and ileum from the posterior wall of the abdomen, and, as the mesocolon, surrounds parts of the colon (meso-appendix, transverse mesocolon, sigmoid mesocolon).

'Peritoneal carcinomatosis' is a term used for extensive metastatic involvement of the inner surfaces of the pelvis and abdomen. This condition is most often encountered in advanced primary ovarian, tubal or peritoneal cancer or endometrial cancer (Figure S31), and it is divided according to the type of peritoneum affected (Figures 14 and 15). For practical purposes, it is useful to distinguish between pelvic and abdominal peritoneal involvement, including omental involvement in the latter as the omentum is the largest peritoneal fold, and to determine the size and density of tumor nodules (Table S7).

With respect to pelvic carcinomatosis, if high-frequency transvaginal probes are used even small discrete metastatic implants on the pelvic peritoneum can be detected (Figure 14)³³. These usually manifest as hypoechoic lesions with newly formed vessels that, in the course of successful cytostatic treatment, decrease in size and become avascular. Types of pelvic carcinomatosis are presented in Figures S32–S34.

In cases of diffuse visceral carcinomatosis, it is important to distinguish between isolated involvement of the rectosigmoid and concomitant involvement of loops of small intestine (Videoclip S7). The peristaltic movements of pelvic intestinal loops (the ileal loops are usually in the pelvis) that are affected by carcinomatosis may remain normal or become sluggish. In the case of sluggish peristalsis due to carcinomatosis, movement of condensed intestinal content, dilatation of the intestinal lumen (over 30 mm) and thickening of the intestinal wall may be observed. The horizontally positioned Kerckring folds in the jejunum are used to distinguish between the jejunum and the ileum (Videoclip S3 (part e)).

As with disseminated carcinomatosis on the surface of the intestine, mesenteric involvement of small intestine, mesorectum and sigmoid mesocolon, in the form of bulky nodules, is also a negative prognostic sign for optimal cytoreduction at the time of surgery (Figure S34b)³⁴.

With respect to abdominal carcinomatosis, a careful transabdominal ultrasound examination can detect all types of peritoneal involvement (Figure 15) with high specificity³⁵. However, due to the lower resolution of transabdominal sonography, miliary dissemination cannot be detected as it would be with a transvaginal or transrectal examination. Carcinomatosis of the parietal peritoneum and omentum are visualized more easily than are mesenteric and visceral carcinomatosis (Figures S35–S37, Videoclip S8). The image quality is usually improved when ascites is present as this acts as an acoustic window (Figure S38, Videoclip S9), but becomes worse when there are matted loops of intestine which hinder visualization of the mesentery or when tumors are advanced and the borders of omental infiltration become indistinguishable from intestinal and/or parietal carcinomatosis.

For clinical purposes it is important to evaluate the location of omental infiltration. The lesser omentum (also known as small omentum or hepatogastric and hepatoduodenal ligaments) is a thin double layer (fold) of peritoneum that extends from the liver to the lesser curvature of the stomach and the beginning of the duodenum (Figure 16). The greater omentum is the largest two-layer peritoneal fold, hanging down from the large

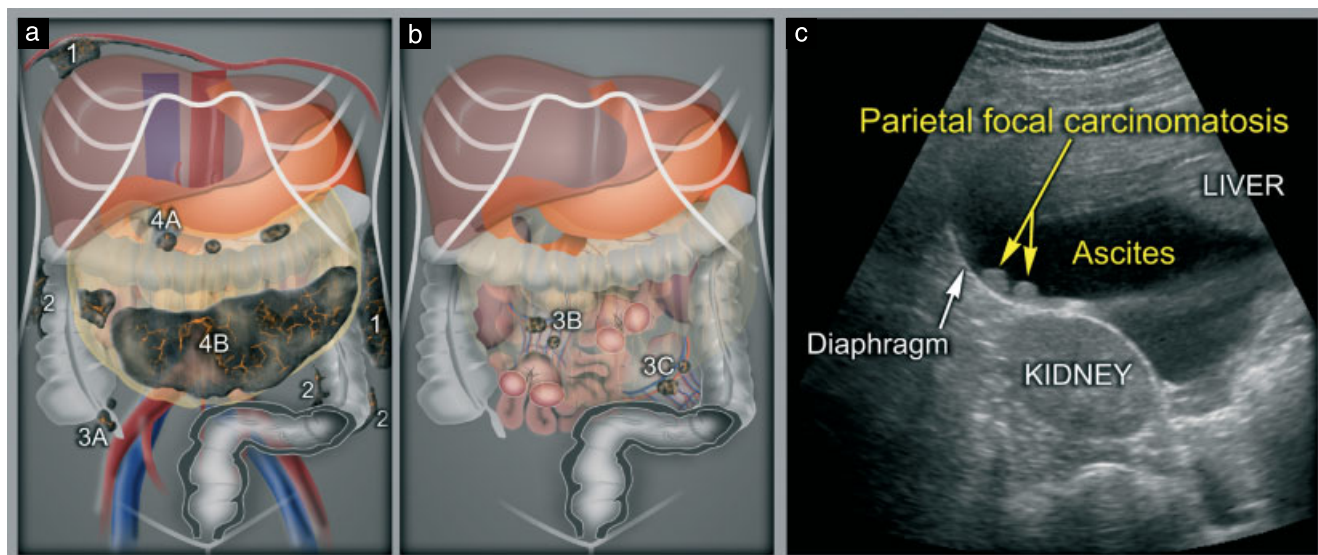


Figure 15 Abdominal carcinomatosis as seen on transabdominal sonography. (a) Schematic diagram showing all types of peritoneal involvement; (b) additional schematic diagram showing mesenteric carcinomatosis. 1, Parietal; 2, visceral; 3, mesenteric (3A, mesoappendix; 3B, mesentery of small intestine; 3C, mesocolon); 4, omental (4A, supracolic omentum; 4B, infracolic omentum). (c) Ultrasound image of diaphragmatic focal nodules.

curvature of the stomach in front of the small intestine, sometimes extending into the pelvis and ascending again to the transverse colon. Its supracolic part is located between the stomach and the transverse colon, while the infracolic part passes from the transverse colon in front of the small intestine. The greater omentum is usually thin and, on ultrasound, has a cribriform hyperechogenic appearance as it contains adipose tissue, which in obese people accumulates in considerable quantities. In the case of tumor spread to the omentum, infiltration may be either focal or diffuse. Focal nodules are found in both the lesser and greater omentum, are hypoechogenic with irregular borders and are vascularized (Figure S37b, Videoclip S10). Diffuse omental infiltration (‘omental cake’) has a characteristic appearance, with a nodular, perfused tumor plate, underneath which the movements of intestinal loops can usually be observed³⁶ (Videoclip S11); if, however, these have already been infiltrated by tumor they are included with the omentum in the ‘matted cake’ (Videoclip S12).

Carcinomatosis is usually accompanied by a large quantity of fluid in the abdominal and peritoneal cavities (Figures S38 and S39), as demonstrated in Videoclip S12, which shows parietal carcinomatosis of the diaphragm and infiltration of the lesser and greater omenta.

LYMPH-NODE INVOLVEMENT (TNM)

An evaluation of the lymph nodes is a critical part of clinical cancer staging that is important for determining prognosis and for selecting optimal treatment. MRI or CT diagnoses of infiltrated lymph nodes are based mainly on their size, with the most widely accepted definition of lymph-node involvement being when the node’s transverse diameter exceeds 10 mm³⁷. Ultrasound differs from these

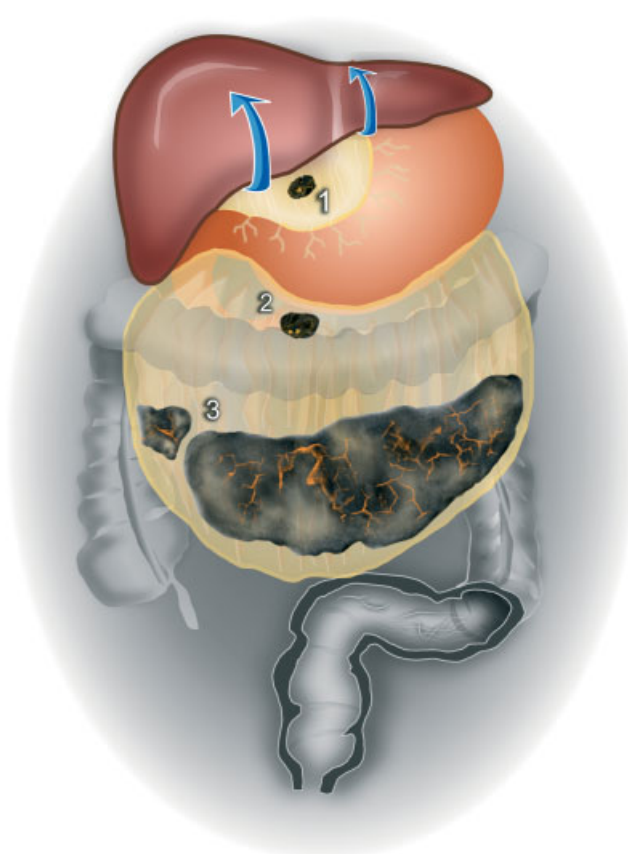


Figure 16 Schematic diagram showing tumor infiltration of lesser omentum and greater omentum, supracolic and infracolic parts. Blue arrows indicate the slight lifting up of the liver that is required to see the lesser omentum. 1, Nodule in the lesser omentum extending from the liver to the lesser curvature of stomach; 2, another nodule in the supracolic omentum close to the transverse colon; 3, infracolic omental cake.

two imaging methods in being able to evaluate accurately the morphology of lymph nodes, allowing identification of changes in their inner structure, especially in infiltrated peripheral lymph nodes. With the use of power Doppler, the vascular pattern of lymph nodes can also be evaluated (Table S8).

The lymph nodes are assessed mainly by transabdominal sonography using a convex-array probe for evaluating deep lymph nodes and a linear-array probe for peripheral lymph nodes. The standard approach for visualizing lymph nodes starts at the inguinal canal and proceeds towards the diaphragm (Figure 17). However, an initial transvaginal or transrectal examination will provide information on the location, size and structure of the ovaries and prevent confusion between a solid small-sized ovary and an infiltrated lymph node. In addition, in some cases, a transvaginal or transrectal examination may visualize lymph nodes in the region of the external iliac vessels and the obturator fossa, as well as the branching of their feeding arteries from large vessels (Figure S40).

Lymph node anatomy and sonographic features

Each lymph node is encapsulated by fibrous tissue and consists of cortical and medullary regions. The cortex is composed of densely packed lymphocytes which group together to form spherical lymphoid follicles (germinal center). The paracortex, an intermediate area between the cortex and the medulla, is a transition area where the lymphocytes return to the lymphatic system from the blood. The main artery enters the lymph node at the hilum, where it branches into arterioles and further into

capillaries to supply the lymphoid follicles in the cortex. The venous system has a similar route to the hilum. In the cortex, the venules converge to form small veins, which further converge to form the main vein in the medulla. The main vein then leaves the lymph node at the hilum (Figure 18).

During immunological processes such as infection or peripheral tumor growth, a lymph node loses its basic structure and proceeds to a reactive state, with characteristic structural changes (Figure 19). This transformation tends to be reversible as long as no neovascularization arises or (micro-) metastases exist within the lymph node (Figure 19)³⁸.

The combination of sonomorphological and vascular patterns of lymph nodes can be used to differentiate metastatic from normal or reactive nodes (Table S8). Normal lymph nodes are bean-shaped with an echogenic medulla, peripheral hypoechoic lymphoid tissue, echogenic capsule and pronounced hyperechoic hilum (Figure S41a)³⁹. On ultrasound, the echogenic hilum appears to be continuous with the adjacent soft tissues (Figure 19d) and a strip of vessels (hilar longitudinal vessels) may be visualized (Figure S41b, Videoclip S13). Normal nodes tend to have only hilar vascularity or appear avascular (Videoclip S14).

Reactive (inflammatory) lymph nodes are oval due to enlargement of reactive centers in the paracortex. There is pronounced hilar perfusion with radial branching from the hilum (Figure 19b and e, Videoclip S15). During the healing process of reactive lymph nodes the echogenic center becomes larger, with lipomatous changes in the sinuses of the medulla (Figure 19h). These changes, together with the presence of only longitudinal hilar vessels, are the

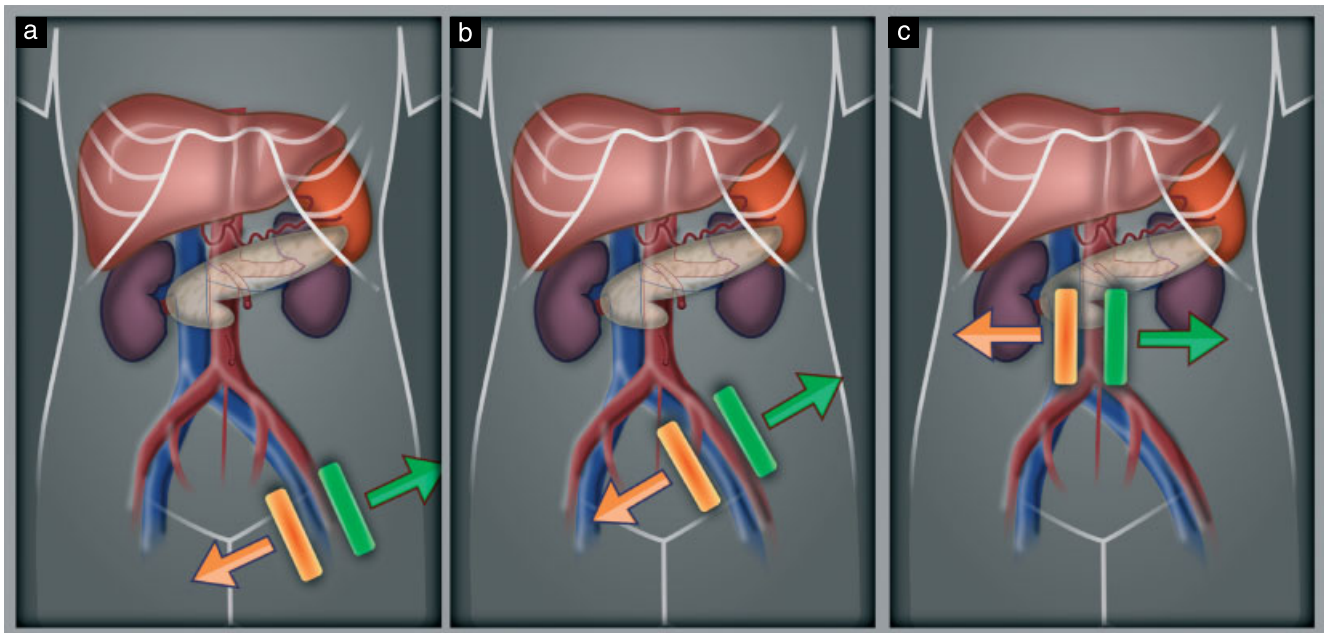


Figure 17 Methodology of lymph node examination from inguinal canal towards periaortic area by transabdominal sonography. (a) Inguinal peripheral lymph node evaluation on the left side; (b) pelvic parietal lymph node evaluation; (c) abdominal parietal lymph node evaluation. Note the movement of the probe (indicated with orange and green bars), which shifts from the inguinal canal upwards to the diaphragm, following the large vessels, concurrent with its slight deviation medially and laterally (orange and green arrows) above the large vessels to assess complete lymphatic drainage.

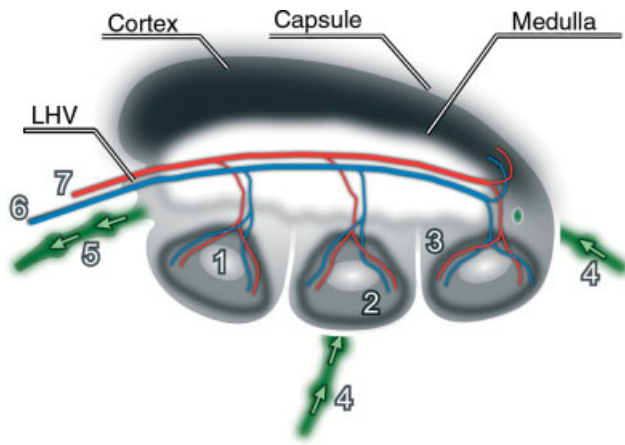


Figure 18 Schematic diagram of a lymph node. 1, Lymphoid follicle; 2, subcapsular sinus; 3, paracortex; 4, afferent lymphatic vessels; 5, efferent lymphatic vessel; 6, vein of node; 7, artery of node; LHV, longitudinal hilar vessels.

basis for the sonographic characteristic appearance of the so-called hilum ‘fat sign’. This sign usually indicates post-reactive but still benign node changes and is found predominantly in peripheral lymph nodes.

An early sign of lymph node involvement by metastasis is peripheral or mixed perfusion (Videoclip S16), which remains in the later stages of metastasis development. Mixed perfusion is predominantly present in lymphomatous nodes³⁹. There may also be focal areas of missing vascularity inside the infiltrated node. In the later stages, the tumor volume expands then undergoes morphological changes. The shape of an infiltrated lymph node is round, with loss of the hilum sign and inhomogeneous echogenicity (Figure S41c). Metastatic nodes of gynecological cancers are usually hypoechogetic⁴⁰. Necrosis, calcification or partial lymph-node infiltration may produce a heterogeneous ultrasound pattern. They can show extracapsular growth with irregular margin and diffuse

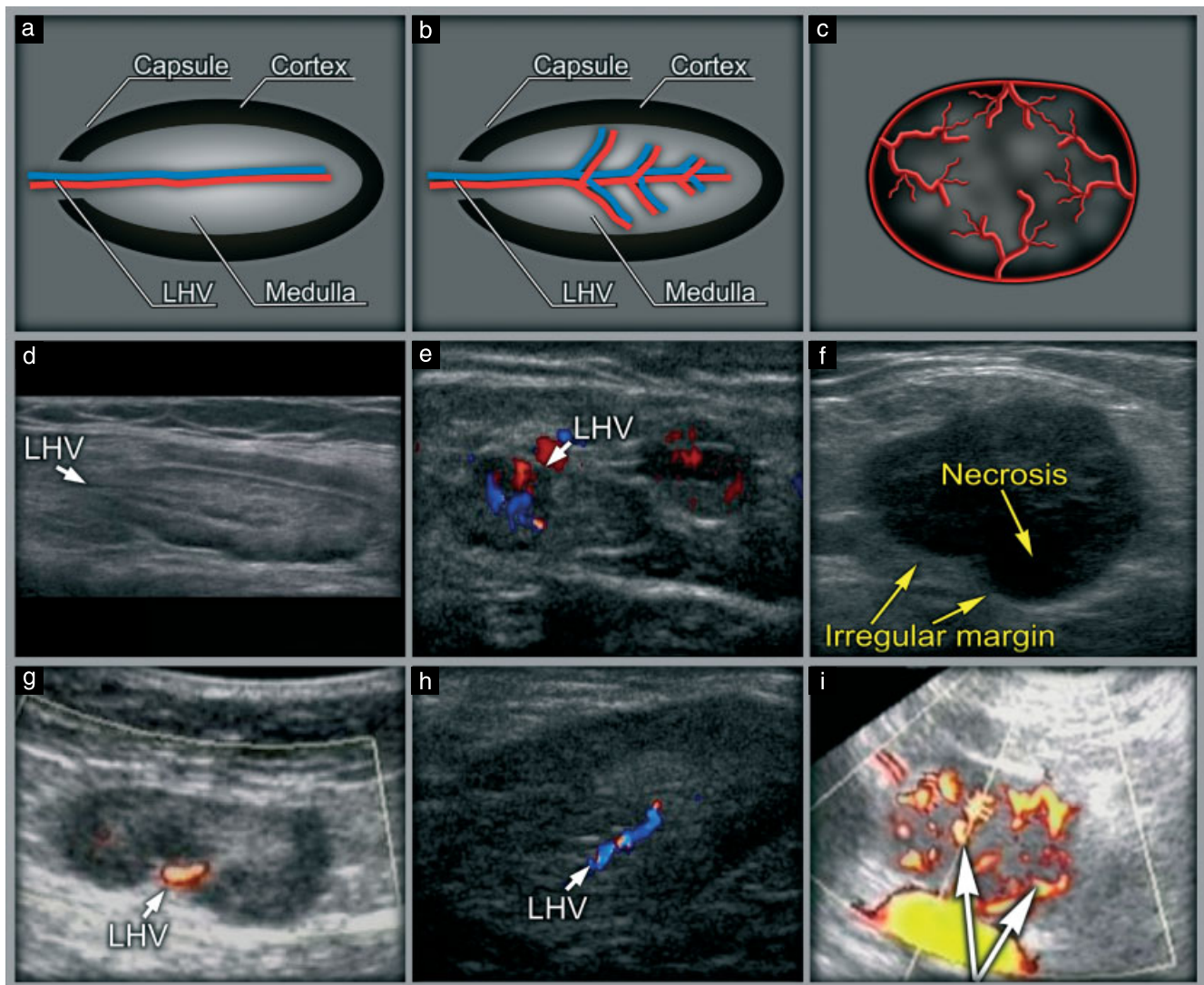


Figure 19 (a–c) Schematic diagrams showing: (a) normal, (b) reactive and (c) infiltrated lymph nodes. (d–i) Ultrasound images showing: (d) echogenic hilum with longitudinal hilar vessel (LHV); (e) radial branching of longitudinal hilar vessels in the reactive lymph node; (f) infiltrated lymph node; (g) normal bean-shaped node with an echogenic medulla and peripheral hypoechogetic lymphoid tissue; (h) post healing lipomatous changes in medulla with hilum fat sign; (i) infiltrated lymph node with peripheral and central (mixed) perfusion (arrows).

infiltrating growth into vessels and surrounding tissue (Figure 19f).

Distribution and classification of lymph nodes

Lymph nodes are divided into peripheral (e.g. superficial and deep inguinal lymph nodes) and non-peripheral lymph nodes (Table S9, Figure 20). The latter group includes parietal lymph nodes, corresponding to the retroperitoneal compartment (periaortic and iliac lymph nodes), and visceral lymph nodes, corresponding to the intraperitoneal compartment. Visceral lymph nodes receive lymph from abdominal organs associated with the visceral branches of the aorta (along the course of the celiac trunk, including lymph nodes of splenic and hepatic hilum and superior and inferior mesenteric vessels) and from pelvic organs.

Peripheral lymph nodes

In gynecological oncology, the peripheral lymph nodes that are especially interesting from a clinical point of view are the inguinal, axillary and scalene lymph nodes (Figure S42), among which particular attention is paid to the inguinal lymph nodes on ultrasound examination

as these are regional nodes for vulval, vaginal and ovarian cancer (Figure S43). Examination of scalene nodes (supraclavicular nodes in proximity to the scalene muscle) is valuable for the detection of disseminated or recurrent malignant gynecological cancers (Figure S44).

Orientation in the inguinal region is helped by visualization of the femoral vessels in the longitudinal plane and, dorsally, of the echogenic structure of the superior ramus of the pubis. To evaluate the superficial and deep inguinal lymph nodes, it is necessary to move the probe medially and laterally in relation to the femoral vein immediately beneath the inguinal canal. The superficial inguinal lymph nodes form a chain and are found in the triangular area bounded by the inguinal ligament superiorly, the border of the sartorius muscle laterally and the adductor longus muscle medially. There are approximately 10 superficial lymph nodes, divided into three groups: superomedial, superolateral (Videoclip S17) and inferior (Figure 21). The deep inguinal lymph nodes, of which there are approximately three to five, are located medial to the femoral vein and underneath the cribriform fascia. The superior (highest) deep inguinal node is located under the inguinal ligament and is called 'Cloquet's node'.

Retroperitoneal lymph nodes

After evaluation of the inguinal lymph nodes, the probe should be moved cranially in an oblique section to evaluate the external iliac artery accompanied by the collapsible external iliac vein, which is located behind the artery on the psoas major muscle (Figure 17b). Beneath the external iliac vessels is the obturator fossa. At the pelvic brim is the bifurcation of the internal and external iliac vessels. The internal iliac artery arises at the bifurcation of the common iliac artery anterior to the internal iliac vein. Moving cranially, the probe follows the common iliac artery running alongside the medial border of the psoas major muscle. At the level of the fourth lumbar

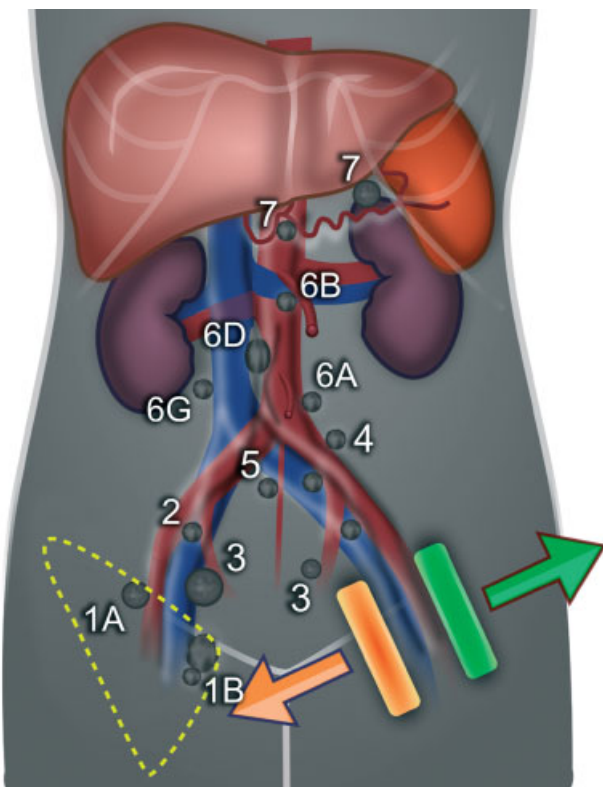


Figure 20 Schematic diagram of lymph node distribution. Arrows indicate probe movement. 1A, Superficial inguinal nodes; 1B, deep inguinal nodes; 2, external iliac nodes; 3, internal iliac nodes; 4, common iliac nodes; 5, sacral nodes (sacral nodes are included among internal iliac nodes); 6A, lateral aortic nodes; 6B, preaortic; 6D, intermediate lumbar nodes; 6G, lateral caval nodes; 7, visceral nodes.

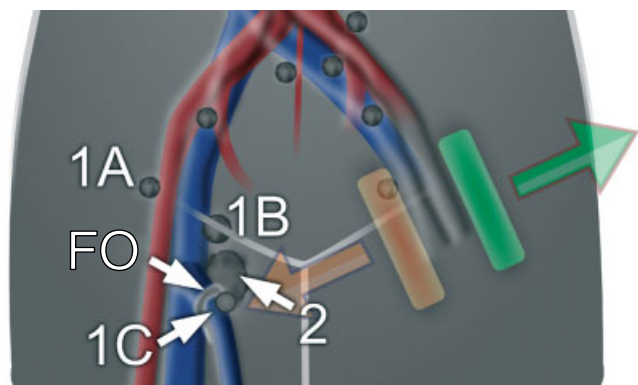


Figure 21 Schematic diagram of inguinal lymph node distribution. 1A, Superficial superolateral inguinal nodes; 1B, superficial superomedial inguinal nodes; 1C, superficial inferior nodes; 2, deep inguinal nodes, which are located medial to the femoral vein under the cribriform fascia. Note the portion of fascia covering the fossa ovalis (FO) perforated by the great saphenous vein accompanied by superficial inferior nodes.

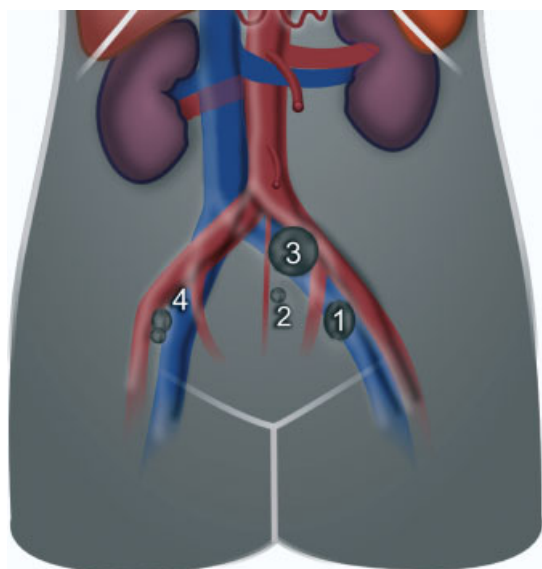


Figure 22 Schematic diagram of parietal pelvic lymph node distribution. 1, External iliac (obturator node); 2, internal iliac (sacral node); 3, common iliac (intermediate node); 4, external iliac (intermediate node).

vertebra below the level of the umbilicus, the aortic bifurcation can be observed, which is the point at which the abdominal aorta bifurcates into the left and right common iliac arteries. The common iliac artery exists as a paired structure. Both common iliac arteries are accompanied along their course by common iliac veins. The right common iliac artery crosses the left common iliac vein anteriorly. The bifurcation of the inferior vena cava is at L5 and, therefore, below the bifurcation of the aorta.

The pelvic parietal lymph nodes are classified according to the Federative Committee on Anatomical Terminology (1998) into the following groups: external iliac (including medial, intermediate, lateral, interiliac and obturator nodes), internal iliac (including gluteal and sacral nodes) and common iliac (including medial, intermediate, lateral, subaortic and promontorial nodes) (Figure 22, Figure S45, Videoclip S18)²⁸.

The abdominal aorta runs parallel and to the left of the inferior vena cava. To examine the periaortic and pericaval lymph nodes, the probe should be moved to obtain the sagittal plane in order to examine from the aortic and caval bifurcation to the diaphragm. Small movements of the probe from left to right and back (Figure 17c) should be used to evaluate the abdominal parietal lymph nodes (left from the aorta: lateral aortic nodes, pre- and postaortic nodes, interaortocaval intermediate lumbar nodes, pre- and postcaval nodes and lateral caval nodes) (Figure 23, Videoclip S19). Based on the branching of the inferior mesenteric artery, the abdominal parietal lymph nodes can be further divided into lower level (inframesenteric – up to branching of inferior mesenteric artery) and upper level (supramesenteric – above branching of inferior mesenteric artery). A disadvantage of ultrasound is that the retroperitoneal (parietal) lymph nodes are more difficult to image in obese patients or in other cases of poor acoustic conditions, such as cases of postsurgical adhesions.

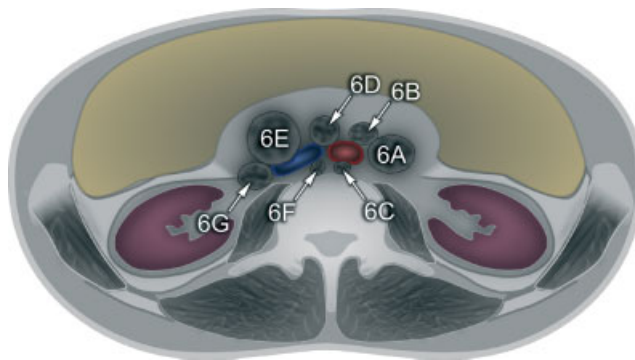


Figure 23 Schematic diagram of abdominal parietal lymph node distribution: left lumbar nodes (6A, lateral aortic; 6B, preaortic; 6C, postaortic); intermediate lumbar nodes (6D); and right lumbar nodes (6E, precaval; 6F, postcaval; 6G, lateral caval). It is important to note that although the ‘para-aortic’ lymph nodes have a special distinction in medical literature as comprising the group of all nodes surrounding the aorta and inferior vena cava, they in fact include only those nodes lateral to the aorta (6A, lateral aortic nodes).

Visceral lymph nodes

The visceral lymph nodes in the pelvis (lateral vesical, pre- and retrovesical, parauterine, paravaginal, pararectal nodes) can be visualized adequately using a transvaginal probe. Furthermore, abdominal infiltrated visceral lymph nodes in the area of the branching of the superior mesenteric artery and the celiac trunk may be visualized well on transabdominal ultrasound and these are often found in advanced ovarian cancer (Figure 24, Figure S46, Videoclip S20).

In gynecological oncology, the most accurate information on the state of the lymph nodes is obtained through systematic surgical staging. Nevertheless, ultrasound has an important role in initial staging. After the primary tumor site is diagnosed, any imaging of lymph nodes will focus on the lymphatic drainage of that particular organ. In malignant tumors of the vulva, ultrasound staging of the inguinofemoral lymph nodes is now established as obligatory. In cervical cancer, ultrasound often detects infiltrated iliac lymph nodes, which modifies any subsequent surgical procedure from being primary radical surgery to a staging procedure. In endometrial cancer, the acoustic conditions for an ultrasound examination of retroperitoneal lymph nodes are often limited due to body habitus. However, these patients, with the exception of low-risk endometrial cancer patients⁴¹, are generally referred for systematic surgical lymph node staging. In ovarian cancer, evaluation of the retroperitoneum may also be hindered by ascites or matted intestinal loops due to carcinomatosis. The advantage of an ultrasound examination in this context lies in its capability to detect accurately inguinofemoral lymphadenopathy that requires resection, in order to achieve optimal cytoreduction, and also for the detection (or exclusion) of bulky lymphadenopathy above the branching of the renal vessels. This area is almost always accessible to a detailed ultrasound examination, and it is usually the presence of

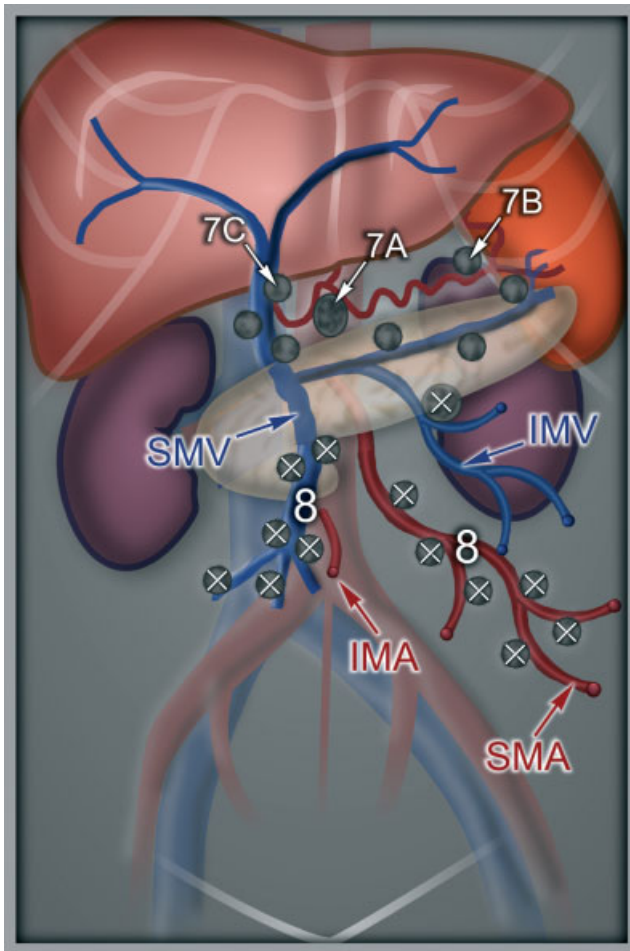


Figure 24 Schematic diagram of visceral lymph node distribution. 7A, Celiac nodes; 7B, splenic nodes; 7C, hepatic nodes along the portal vein; 8, superior and inferior mesenteric nodes; IMA, inferior mesenteric artery; IMV, inferior mesenteric vein; SMA, superior mesenteric artery; SMV, superior mesenteric vein. Note that the abdominal visceral lymph nodes accompany the visceral branches of the celiac trunk and the superior and inferior mesenteric artery and vein.

bulky (> 2 cm) lymphadenopathy of visceral or retroperitoneal lymph nodes above the branching of the renal vessels that prevents a complete cytoreductive procedure. It is not unusual, in patients who are referred for a gynecological oncology assessment with suspected ovarian tumor, to find bulky retroperitoneal lymphadenopathy due to malignant hematological disease with uninvolved ovaries *in situ*. Hodgkin's lymphoma located in the retroperitoneal space often surrounds or dislodges adjacent vessels but does not infiltrate them. In non-Hodgkin lymphomas, usually the mesenteric lymph nodes are involved (Videoclip S21).

DISTANT METASTASES (TNM)

Distant metastases detected by ultrasound most often present as hematogenous spread to the visceral organs (Figure 25, Videoclip S12). Growth of superficial metastatic implants through the capsule of the organ into its parenchyma, or through serosa into the lumen

of intestinal loops, is also considered distant metastatic disease. Also, the involvement of the extrapelvic peritoneum is considered to be distant metastatic spread (TNM1), as demonstrated in Videoclip S12, while the advanced ovarian, tubal and peritoneal tumors with involvement of the extrapelvic peritoneum are not considered as distant metastases. The tumor could also spread lymphatically from regional lymph nodes to the collecting lymph nodes, such involvement also being considered distant metastasis (e.g. infiltrated inguinal lymph nodes in cervical or endometrial cancer, infiltrated iliac lymph nodes in vulval cancer, infiltrated para-aortic lymph nodes in cervical cancer). This section will focus on hematogenous metastases as the other distant metastases have been discussed above.

Liver metastases

Ultrasound is the initial examination method of choice in cases of suspected metastatic involvement of the liver. The liver is evaluated first in the sagittal view, in the right, middle and left medioclavicular lines, and then in the subcostal, transverse and finally the intercostal oblique views (Figure 26).

Secondary tumors (metastatic involvement) are the most common malignant liver tumors. The ultrasound-based morphological characteristics of a metastasis involve its size, type of primary tumor and secondary changes of lesions (e.g. hemorrhage, necrosis, calcification, scarring). Small metastases are homogeneous, but with growth and regression they change; thus, liver metastases vary in their echogenicity according to how long they have been *in situ*. Hypoechoic metastases (Figure S47a–c) are more commonly encountered. The hypoechoicity is due to the relatively high water content in tumor tissue compared with the surrounding normal liver parenchyma. This, however, changes in cases of liver steatosis (fatty liver), when virtually all focal lesions appear hypoechoic. As the metastasis progresses, the echogenicity increases centrally, with a hypoechoic zone remaining on the periphery (halo sign, target lesion, bull's eye sign). This is associated with rapid growth of tumor tissue (proliferation zone), with a high density of newly formed vessels (Figure S47d). Hyperechoic metastases are found, for example, in carcinoids and bronchogenic and renal carcinomas (Figure S47e, Videoclip S22). These are richly vascularized metastases similar to those seen in breast cancer, lymphomas and melanomas. In the center of rapidly growing metastases, necrosis often occurs (presenting as a centrally located anechoic area) and this may lead to an increased acoustic signal similar to the enhancement that occurs behind a benign cyst. Degenerative cystic changes of the tumor center may be followed by a secondary infection or an abscess.

Metastases can be solitary (Figure S47a), multiple (Figure S47b) or present as a diffuse infiltration of the liver parenchyma (Figure S47c). Small lesions usually have distinct borders; with growth, however, the surrounding

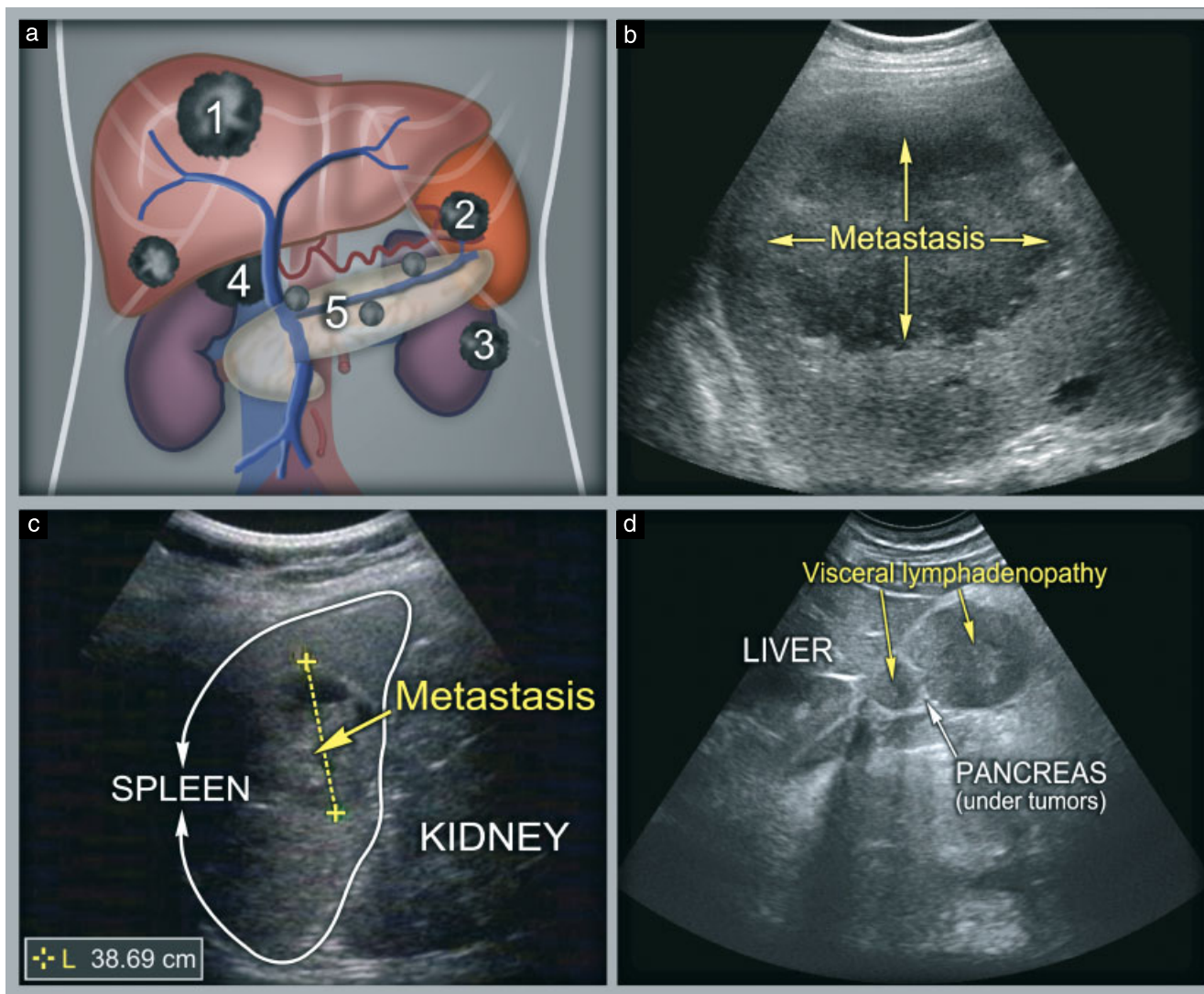


Figure 25 (a) Schematic diagram of metastatic involvement of visceral organs. 1, Liver; 2, spleen; 3, kidney; 4, suprarenal gland; 5, pancreas. (b–d) Ultrasound images showing: (b) hypoechoogenic large metastasis with irregular margin in right lobe of the liver; (c) solid, partially necrotic metastasis in the spleen; (d) tumor nodules surrounding the pancreas in the form of visceral carcinomatosis. Note that metastatic involvement of the pancreas is very rare; often, however, the surrounding area is affected by lymph node metastases, which can give the impression of the pancreas also being infiltrated.

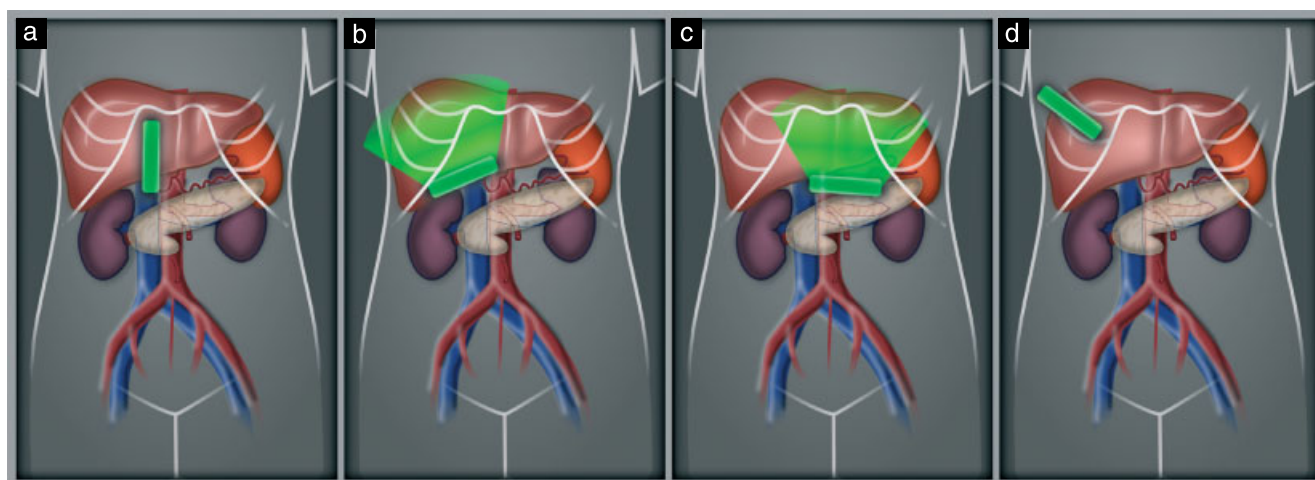


Figure 26 Schematic diagrams of liver examination by transabdominal ultrasound, showing position of the probe to obtain: (a) sagittal section, (b) subcostal section, (c) transverse section and (d) intercostal oblique view.

liver tissue is infiltrated and the lesions become less clearly demarcated. A typical sign of malignancy is an infiltrative penetration into vessels, biliary pathways and surrounding organs. The size of metastatic lesions varies from several millimeters to up to 20 cm. Most often, multiple confluent lesions that epitomize the term 'metastatic liver' (Videoclip S23) are encountered.

The usefulness of ultrasound in assessment of the liver is limited when there are small (< 10 mm) or isoechoic lesions (Figure S47f), or unsatisfactory acoustic conditions in obese and/or non-compliant patients. Cytostatic therapy also changes the echogenicity of the lesions and, for evaluation of the impact of chemotherapy, contrast-enhanced ultrasonography is preferred.

Metastatic involvement of other visceral organs and suprarenal glands

In the spleen, as in the liver, hemangiomas or cysts that do not require further imaging are not uncommon; in cases of

less typical focal or diffuse involvement, complementary imaging methods are required (Figure S48, Videoclip S24, Figure 27).

Hematogenous spread of gynecological tumors to the kidney is rare; however, in view of the increasing incidence of bilateral renal carcinoma, the renal parenchyma should always be examined carefully (Figure S49, Figure 28). Gynecological tumors may also spread in the form of implant metastases on the renal capsule (Figure S50). Richly vascularized hematogenic metastases are more often encountered in the suprarenal glands (Figure S51).

The pancreas is easily accessible to ultrasound examination; it is often surrounded by visceral lymphadenopathy along the course of the splenic artery or the superior mesenteric artery, which can be falsely interpreted as a primary pancreatic cancer (Figures 29 and 25d, Videoclip S20).

If a normal visceral organ or characteristic diffuse or focal lesions (such as a simple cyst, hepatic hemangioma, renal angiomyolipoma, fatty liver (steatosis)) are identified on ultrasound, additional examinations using complementary imaging methods are not required. If, however, less characteristic findings are encountered, especially when the examination result affects radically subsequent therapeutic management, an additional examination using a complementary imaging method (e.g. contrast-enhanced ultrasound, CT, MRI, positron emission tomography) is indicated.

ACKNOWLEDGMENTS

Thanks to Adam Preisler from the Faculty of Architecture, Czech Technical University, Prague, for providing the illustrations and to Tomas Herrmann of the Scientific Headquarters of Information, First Faculty of Medicine, Charles University, Prague, for editing the videoclips.

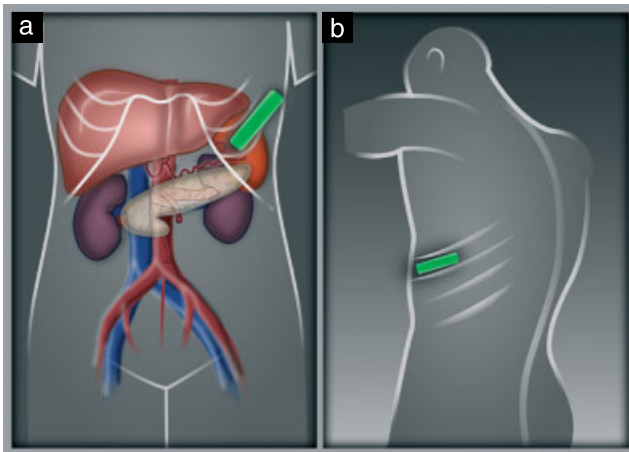


Figure 27 Schematic diagrams showing transabdominal ultrasound examination of the spleen in the left transcostal oblique plane: frontal (a) and side (b) views. The patient is examined in a supine position or is asked to roll onto her right side.

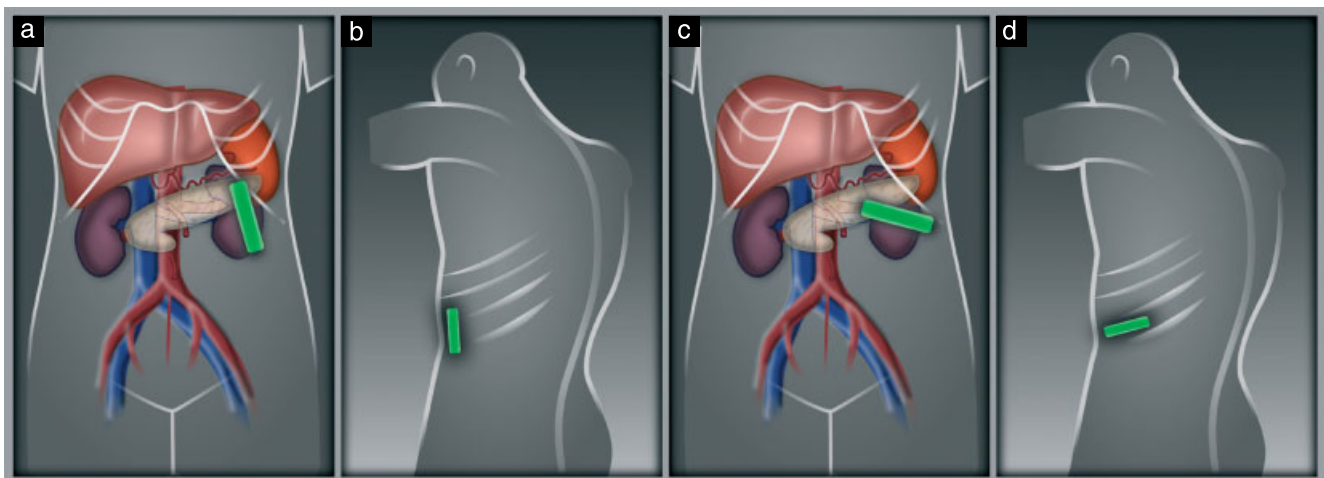


Figure 28 Schematic diagrams of kidney examination by ultrasound, showing position of the probe. (a) Examination of the left kidney in the left sagittal section; (b) side view; (c) the probe is turned 90° counterclockwise to observe the transverse section of the left kidney; (d) side view. Note that, as for the left side, ultrasound is performed on the right upper quadrant of the abdomen to evaluate the right kidney.

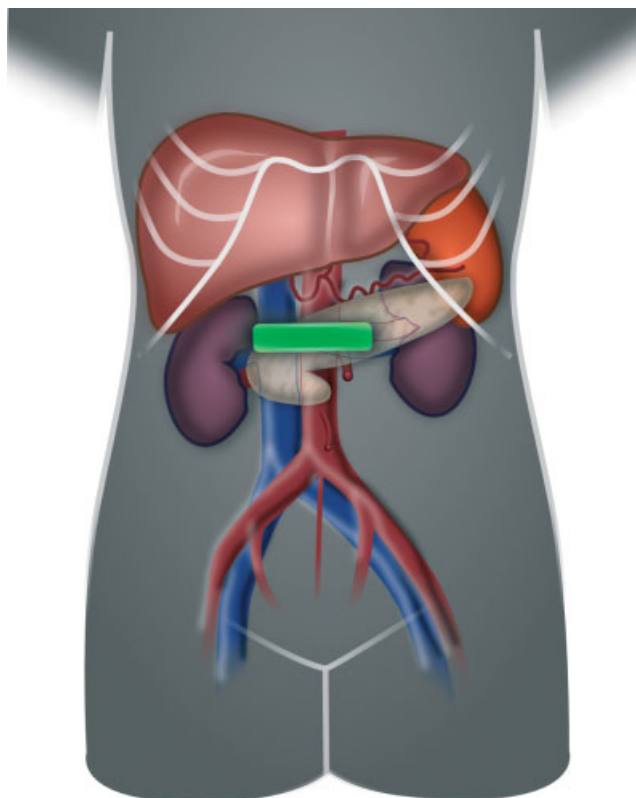


Figure 29 Schematic diagram of pancreas examination by ultrasound, showing position of the probe. This is the final organ to be evaluated, and is located in the epigastrium. It is examined in transverse view on ultrasound.

REFERENCES

1. Fischerova D, Cibula D, Dundr P, Zikan M, Calda P, Freitag P, Slama J. Ultrasound-guided tru-cut biopsy in the management of advanced abdomino-pelvic tumors. *Int J Gynecol Cancer* 2008; **18**: 833–837.
2. Testa AC, Van Holsbeke C, Mascilini F, Timmerman D. Dynamic and interactive gynecological ultrasound examination. *Ultrasound Obstet Gynecol* 2009; **34**: 225–229.
3. Alcázar JL, Castillo G, Jurado M, López-García G. Intratumoral blood flow in cervical cancer as assessed by transvaginal color Doppler ultrasonography: Correlation with tumor characteristics. *Int J Gynecol Cancer* 2003; **13**: 510–514.
4. Cheng WF, Wei LH, Su YN, Cheng SP, Chu JS, Lee CN. The possible use of colour flow Doppler in planning treatment in early invasive carcinoma of the cervix. *Br J Obstet Gynaecol* 1999; **106**: 1137–1142.
5. Testa AC, Ferrandina G, Distefano M, Fruscella E, Mansueti D, Basso D, Salutati V, Scambia G. Color Doppler velocimetry and three-dimensional color power angiography of cervical carcinoma. *Ultrasound Obstet Gynecol* 2004; **24**: 445–452.
6. Testa AC, Ciampelli M, Mastromarino C, Lopez R, Zannoni G, Ferrandina G, Scambia G. Intratumoral color Doppler analysis in endometrial carcinoma: is it clinically useful? *Gynecol Oncol* 2003; **88**: 298–303.
7. Timmerman D, Valentin L, Bourne TH, Collins WP, Verrelst H, Vergote I; International Ovarian Tumor Analysis (IOTA) Group. Terms, definitions and measurements to describe the sonographic features of adnexal tumors: a consensus opinion from the International Ovarian Tumor Analysis (IOTA) Group. Review. *Ultrasound Obstet Gynecol* 2000; **16**: 500–505.
8. Seitz K, Strobel D, Bernatik T, Blank W, Friedrich-Rust M, Herbay A, Dietrich CF, Strunk H, Kratzer W, Schuler A.

- Contrast-Enhanced Ultrasound (CEUS) for the characterization of focal liver lesions – prospective comparison in clinical practice: CEUS vs. CT (DEGUM multicenter trial). *Ultraschall Med* 2009; **30**: 383–389.
9. Benedet JL, Bender H, Jones H 3rd, Ngan HY, Pecorelli S. FIGO staging classifications and clinical practice guidelines in the management of gynecologic cancers. FIGO Committee on Gynecologic Oncology. *Int J Gynaecol Obstet* 2000; **70**: 209–262.
10. International Union Against Cancer (UICC). *TNM Classification of Malignant Tumours*, 7th edn. Sobin LH, Gospodarowicz MK, Wittekind C (eds.) John Wiley & Sons: New York, 2009; ISBN 978-1-4443-3241-4.
11. Pecorelli S. Revised FIGO staging for carcinoma of the vulva, cervix, and endometrium. *Int J Gynaecol Obstet* 2009; **105**: 103–104.
12. Fischerova D, Cibula D, Stenhova H, Vondrichova H, Calda P, Zikan M, Freitag P, Slama J, Dundr P, Belacek J. Transrectal ultrasound and magnetic resonance imaging in staging of early cervical cancer. *Int J Gynecol Cancer* 2008; **18**: 766–772.
13. Testa AC, Ludovisi M, Manfredi R, Zannoni G, Gui B, Basso D, Di Legge A, Licameli A, Di Bidino R, Scambia G, Ferrandina G. Transvaginal ultrasonography and magnetic resonance imaging for assessment of presence, size and extent of invasive cervical cancer. *Ultrasound Obstet Gynecol* 2009; **34**: 335–344.
14. Gaurilcik A, Vaitkiene D, Cizauskas A, Inciura A, Svedas E, Maciuleviciene R, Di Legge A, Ferrandina G, Testa AC, Valentin L. Early-stage cervical cancer: agreement between ultrasound and histopathological findings with regard to tumor size and extent of local disease. *Ultrasound Obstet Gynecol* 2011; DOI: 10.1002/uog.9037.
15. Innocenti P, Pulli F, Savino L, Nicolucci A, Pandimiglio A, Menchi I, Massi G. Staging of cervical cancer: reliability of transrectal US. *Radiology* 1992; **185**: 201–205.
16. Fischerova D, Cibula D, Zikan M, Pinkavova I, Dundr P, Calda P. Role of ultrasound in the referral of young patients with cervical cancer for fertility sparing surgery (OC 23.01). *Ultrasound Obstet Gynecol* 2009; **34** (Suppl 1) 43.
17. Cibula D, Slama J, Svarovsky J, Fischerova D, Freitag P, Zikan M, Pinkavova I, Pavlista D, Dundr P, Hill M. Abdominal radical trachelectomy in fertility sparing treatment of early-stage cervical cancer. *Int J Gynecol Cancer* 2009; **19**: 1407–1411.
18. Rob L, Skapa P, Robova H. Fertility-sparing surgery in patients with cervical cancer. *Lancet Oncol* 2011; **12**: 192–200.
19. Fischerova D, Cibula D, Calda P, Dundr P, Slama J, Pinkavova I. Role of ultrasound in guiding of surgery radicality in cervical cancer management (OC 129). *Ultrasound Obstet Gynecol* 2008; **32**: 285.
20. Leone FP, Timmerman D, Bourne T, Valentin L, Epstein E, Goldstein SR, Marret H, Parsons AK, Gull B, Istre O, Sepulveda W, Ferrazzi E, Van den Bosch T. Terms, definitions and measurements to describe the sonographic features of the endometrium and intrauterine lesions: a consensus opinion from the International Endometrial Tumor Analysis (IETA) group. *Ultrasound Obstet Gynecol* 2010; **35**: 103–112.
21. Karlsson B, Norström A, Granberg S, Wikland M. The use of endovaginal ultrasound to diagnose invasion of endometrial carcinoma. *Ultrasound Obstet Gynecol* 1992; **2**: 35–39.
22. Weber G, Merz E, Bahlmann F, Mitze M, Weikel W, Knapstein PG. Assessment of myometrial infiltration and preoperative staging by transvaginal ultrasound in patients with endometrial carcinoma. *Ultrasound Obstet Gynecol* 1995; **6**: 362–367.
23. Savelli L, Ceccarini M, Ludovisi M, Fruscella E, De Iaco PA, Salizzoni E, Mabrouk M, Manfredi R, Testa AC, Ferrandina G. Preoperative local staging of endometrial cancer: transvaginal sonography vs. magnetic resonance imaging. *Ultrasound Obstet Gynecol* 2008; **31**: 560–566.
24. Lindauer J, Fowler JM, Manolitsas TP, Copeland LJ, Eaton LA, Ramirez NC, Cohn DE. Is there a prognostic difference between

- depth of myometrial invasion and the tumor-free distance from the uterine serosa in endometrial cancer? *Gynecol Oncol* 2003; **91**: 547–551.
25. Creasman WT, Morrow CP, Bundy BN, Homesley HD, Graham JE, Heller PB. Surgical pathologic spread patterns of endometrial cancer. A Gynecologic Oncology Group Study. *Cancer* 1987; **60** (Suppl 8) 2035–2041.
 26. Epstein E, van Holsbeke C, Mascilini F, Måsbäck A, Kanisto P, Ameye L, Fischerova D, Zannoni GF, Vellone V, Timmerman D, Testa AC. Gray-scale and color Doppler ultrasound characteristics of endometrial cancer in relation to stage, grade and tumor size. *Ultrasound Obstet Gynecol* 2011; DOI: 10.1002/uog.9038.
 27. Timmerman D, Van Calster B, Testa AC, Guerriero S, Fischerova D, Lissoni AA, Van Holsbeke C, Fruscio R, Czekierdowski A, Jurkovic D, Savelli L, Vergote I, Bourne T, Van Huffel S, Valentin L. Ovarian cancer prediction in adnexal masses using ultrasound-based logistic regression models: a temporal and external validation study by the IOTA group. *Ultrasound Obstet Gynecol* 2010; **36**: 226–234.
 28. Federative Committee on Anatomical Terminology. *Terminologia Anatomica*. Georg Thieme Verlag: Stuttgart, 1998; (ISBN 3-13-115251).
 29. Ercoli A, Delmas V, Fanfani F, Gadonneix P, Ceccaroni M, Fagotti A, Mancuso S, Scambia G. Terminologia Anatomica versus unofficial descriptions and nomenclature of the fasciae and ligaments of the female pelvis: a dissection-based comparative study. *Am J Obstet Gynecol* 2005; **193**: 1565–1573.
 30. Querleu D, Morrow CP. Classification of radical hysterectomy. Review. *Lancet Oncol* 2008; **9**: 297–303.
 31. Cibula D, Abu-Rustum NR, Benedetti-Panici P, Köhler C, Raspagliesi F, Querleu D, Morrow CP. New classification system of radical hysterectomy: Emphasis on a three-dimensional anatomic template for parametrial resection. *Gynecol Oncol* 2011; **122**: 264–268.
 32. Iwamoto K, Kigawa J, Minagawa Y, Miura H, Terakawa N. Transvaginal ultrasonographic diagnosis of bladder-wall invasion in patients with cervical cancer. *Obstet Gynecol* 1994; **83**: 217–219.
 33. Savelli L, De Iaco P, Ceccaroni M, Ghi T, Ceccarini M, Seracchioli R, Cacciatore B. Transvaginal sonographic features of peritoneal carcinomatosis. *Ultrasound Obstet Gynecol* 2005; **26**: 552–557.
 34. Fischerova D, Cibula D, Dunder P, Zikan M, Freitag P, Slama J, Calda P. The role of ultrasound in prediction of optimal vs suboptimal cytoreductive surgery in advanced ovarian cancers (OC 132). *Ultrasound Obstet Gynecol* 2008; **32**: 286.
 35. Kurtz AB, Tsimikas JV, Tempany CM, Hamper UM, Arger PH, Bree RL, Wechsler RJ, Francis IR, Kuhlman JE, Siegelman ES, Mitchell DG, Silverman SG, Brown DL, Sheth S, Coleman BG, Ellis JH, Kurman RJ, Caudry DJ, McNeil BJ. Diagnosis and staging of ovarian cancer: comparative values of Doppler and conventional US, CT, and MR imaging correlated with surgery and histopathologic analysis—report of the Radiology Diagnostic Oncology Group. *Radiology* 1999; **212**: 19–27.
 36. Testa AC, Ludovisi M, Savelli L, Fruscella E, Ghi T, Fagotti A, Scambia G, Ferrandina G. Ultrasound and color power Doppler in the detection of metastatic omentum: a prospective study. *Ultrasound Obstet Gynecol* 2006; **27**: 65–70.
 37. Nicolet V, Carignan L, Bourdon F, Prosmann O. MR imaging of cervical carcinoma: a practical staging approach. Review. *Radiographics* 2000; **20**: 1539–1549.
 38. Voit C, Van Akkooi AC, Schäfer-Hesterberg G, Schoengen A, Kowalczyk K, Roewert JC, Sterry W, Eggermont AM. Ultrasound morphology criteria predict metastatic disease of the sentinel nodes in patients with melanoma. *J Clin Oncol* 2010; **28**: 847–852.
 39. Ahuja AT, Ying M. Sonographic evaluation of cervical lymph nodes. Review. *AJR Am J Roentgenol* 2005; **184**: 1691–1699.
 40. Hall TB, Barton DP, Trott PA, Nasiri N, Shepherd JH, Thomas JM, Moskovic EC. The role of ultrasound-guided cytology of groin lymph nodes in the management of squamous cell carcinoma of the vulva: 5-year experience in 44 patients. *Clin Radiol* 2003; **58**: 367–371.
 41. Hernandez E; American College of Obstetricians and Gynecologists. ACOG Practice Bulletin number 65: management of endometrial cancer. *Obstet Gynecol* 2006; **107**: 952; author reply: 952.

SUPPORTING INFORMATION ON THE INTERNET



Videoclips S1–S24, Figures S1–S51 and Tables S1–S9 may be found in the online version of this article.